© 2021. Published by The Company of Biologists Ltd | Development (2021) 148, dev187534. doi:10.1242/dev.187534

STEM CELLS AND REGENERATION

RESEARCH ARTICLE

Mechanosensory neuron regeneration in adult *Drosophila*

Ismael Fernández-Hernández[1,*], Evan B. Marsh[1] and Michael A. Bonaguidi[1,2,3,4,*]

ABSTRACT

Auditory and vestibular mechanosensory hair cells do not regenerate following injury or aging in the adult mammalian inner ear, inducing irreversible hearing loss and balance disorders for millions of people. Research on model systems showing replacement of mechanosensory cells can provide mechanistic insights into developing new regenerative therapies. Here, we developed lineage tracing systems to reveal the generation of mechanosensory neurons in the Johnston's organ (JO) of intact adult *Drosophila*, which are the functional counterparts to hair cells in vertebrates. New JO neurons develop cilia and target central brain circuitry. Unexpectedly, mitotic recombination clones point to JO neuron self-replication as a likely source of neuronal plasticity. This mechanism is further enhanced upon treatment with experimental and ototoxic compounds. Our findings introduce a new platform to expedite research on mechanisms and compounds mediating mechanosensory cell regeneration, with nascent implications for hearing and balance restoration.

KEY WORDS: Regeneration, Nervous system, Auditory neuron, Vestibular neuron, Lineage tracing, *In vivo* imaging

INTRODUCTION

Hearing and balance disorders affect over 5% of the world's population, with one in three people affected by the age of 80 (Geleoc and Holt, 2014). By the year 2050, 900 million people are expected to have hearing and balance disorders (World Health Organization 2020, https://www.who.int/health-topics/hearing-loss#tab=tab_2). These disorders are due to the degeneration of mechanosensory hair cells and their innervating neurons in the inner ear, following damage by genetic mutations, excessive noise, ototoxic drugs or aging. Unfortunately, no treatments exist to replenish lost cells in the human sensory epithelia (Müller and Barr-Gillespie, 2015). Thus, regenerative strategies are urgently needed to recover auditory and vestibular function for millions of people. Although non-mammalian vertebrates are able to functionally replenish hair cells throughout life (Kniss et al., 2016; Ryals et al., 2013; Stone and Cotanche, 2007), mammals show scarce regenerative capacity in the cochlea at early postnatal stages (Bramhall et al., 2014; Cox et al., 2014; Kelley et al., 1995; White et al., 2006) and low levels in vestibular organs during adulthood (Bucks et al., 2017; Forge et al., 1993; Golub et al., 2012; Kawamoto et al., 2009; Warchol et al., 1993). In all cases, non-sensory supporting cells trans-differentiate to regenerate hair cells (Atkinson et al., 2015; Bucks et al., 2017; Kniss et al., 2016; Stone and Cotanche, 2007; White et al., 2006). Still, research on these models at the genetic, cellular, circuitry and behavioral levels is costly and technically challenging.

The fruit fly *Drosophila melanogaster* harbors ciliated mechanosensory neurons in the Johnston's organ (JO) on the second segment of its two antennae. JO neurons are clustered in ∼200 scolopidia per antenna, comprising multicellular units with two or three JO neurons and surrounding supporting cells (Albert and Göpfert, 2015; Boekhoff-Falk and Eberl, 2014; Ishikawa and Kamikouchi, 2016). JO neurons develop in response to conserved genetic programs and act as counterparts to mammalian hair cells and their innervating neurons by supporting auditory and vestibular functions (Boekhoff-Falk, 2005; Eberl and Boekhoff-Falk, 2007; Kamikouchi et al., 2009; Li et al., 2018; Sun et al., 2009; Wang et al., 2002). *Drosophila* represents a compelling platform to accelerate research on the functional regeneration of mechanosensory cells, due to the availability of genome-wide genetic tools; the detailed characterization of JO neurons at the circuitry and behavioral levels (Ishikawa et al., 2017; Kamikouchi et al., 2006; Lai et al., 2012; Matsuo et al., 2016; Vaughan et al., 2014); and simple scalability at low cost. Even so, turnover of JO neurons has not yet been reported. Previous reports demonstrate a proliferative capacity in the brain of adult *Drosophila*, both in physiological conditions and following injury (Fernández-Hernández et al., 2013; Kato et al., 2009; Li et al., 2020). Therefore, we hypothesized that the peripheral nervous system also has this capacity for proliferation. To test this, we implemented multiple modified lineage tracing systems to reveal adult-born JO neurons by longitudinal live imaging of intact adult *Drosophila*. We observed that new JO neurons acquire features of mature, functional neurons. Clones generated through mitotic recombination suggest low frequency self-renewal of JO neurons as a newly discovered mechanism that counteracts neuronal cell death. Furthermore, the oral administration of drugs accelerates this regenerative mechanism within intact flies. Our results underscore the broad potential of this new *in vivo* platform for understanding and promoting mechanosensory cell regeneration.

RESULTS

P-MARCM detects adult neurogenesis in *Drosophila* brain

We previously developed a Perma-Twin system to detect low levels of cell proliferation and regeneration in the adult *Drosophila* brain (Fernández-Hernández et al., 2013). However, this method required antibodies to assess the identity of new cells (e.g. Elav for neurons); also, quantification of new cells relied upon resolving cells labeled only by cytoplasmic fluorescent reporters. Furthermore, this method did not permit the genetic manipulation of adult-born cells. In order to overcome these limitations and detect low levels of cell proliferation in adult *Drosophila* in a cell type-specific and sustained manner, we developed permanent mosaic analysis with a

[1]Department of Stem Cell Biology and Regenerative Medicine, Eli and Edythe Broad Center for Regenerative Medicine and Stem Cell Research, Keck School of Medicine, University of Southern California, Los Angeles, CA 90033, USA. [2]Department of Biomedical Engineering, Viterbi School of Engineering, University of Southern California, Los Angeles, CA 90089, USA. [3]Department of Gerontology, Davis School of Gerontology, University of Southern California, Los Angeles, CA 90089, USA. [4]Zilkha Neurogenetic Institute, Keck School of Medicine, University of Southern California, Los Angeles, CA 90033 USA.

*Authors for correspondence (ismaelfe@usc.edu; mbonagui@usc.edu)

I.F.-H., 0000-0001-9833-919X; M.A.B., 0000-0002-9295-4762

Handling Editor: Thomas Lecuit
Received 17 December 2019; Accepted 9 February 2021

Development (2021) 148, dev187534. doi:10.1242/dev.187534

repressible cell marker (P-MARCM). Built into MARCM (Lee and Luo, 1999), P-MARCM can detect sporadic mitotic events in virtually any adult tissue, and label newly generated cell populations. To activate P-MARCM, a heat shock (HS)-induced pulse of Flippase (FLP) excises an FRT-flanked STOP codon between a *tub* promoter and the transactivator *lexA* (Singh et al., 2013), which in turn binds to the *lexAOp-Flp* sequence (Pfeiffer et al., 2010) to drive Flippase permanently in heat shock-responding cells (Fig. 1A,B). Cell-type specificity is achieved by incorporating desired *GAL4* lines to express nuclear-localized RFP (Barolo et al., 2004) and cytoplasmic GFP (Shearin et al., 2014) only in adult-born cells of interest in a given lineage, making antibodies dispensable to assess cell identity (Lee et al., 2018). These enhanced fluorescent reporters allow for the concurrent assessment of detailed morphology and straight-forward cell quantification. Furthermore, the introduction of an additional UAS-transgene permits genetic manipulation of adult-born cells and assessment of their functional contributions (Fig. 1C). To benchmark the utility of P-MARCM, we used a pan-neuronal *nsyb-GAL4* line and detected previously reported physiological neurogenesis in the adult optic lobes, where we also detected pH3^{+} cells (Fig. S1), and neuronal regeneration upon injury (Fig. S2) (Fernández-Hernández et al., 2013). Therefore, P-MARCM can capture adult cell proliferation in a cell type-specific manner under both physiological and injury conditions.

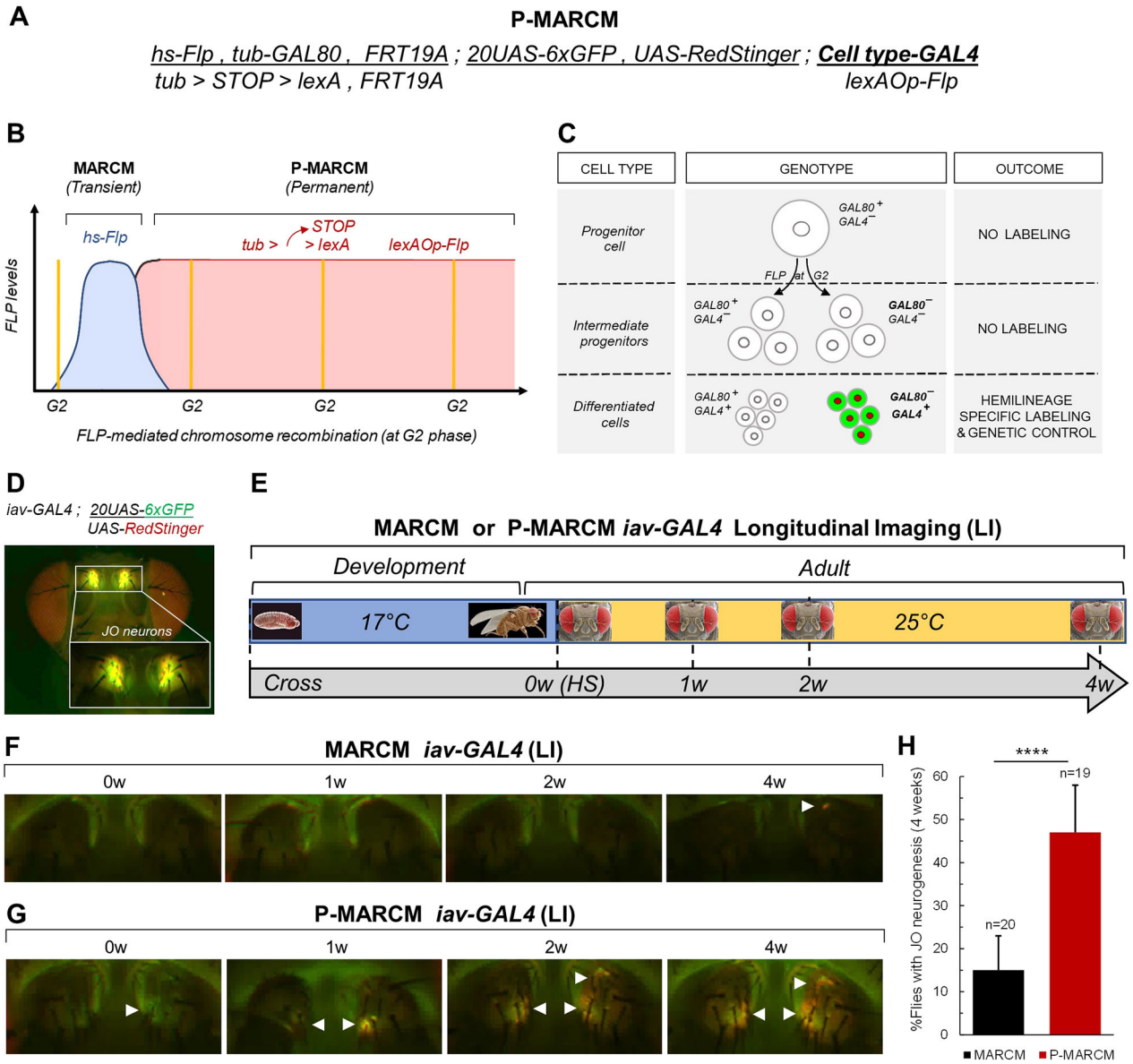

Fig. 1. P-MARCM live imaging reveals JO neurogenesis in adult *Drosophila*. (A) The P-MARCM system used to label and genetically manipulate adult-born cells in a cell type-specific manner. (B) P-MARCM becomes permanently active via constitutive Flippase (FLP)-mediated mitotic chromosome recombination to capture slowly dividing cells. (C) P-MARCM labels adult-born cells of interest in a lineage by cell type-specific *GAL4* lines (*iav-GAL4* for JO neurons). Engineered nuclear red and membrane green fluorescent reporters allows quantification and cellular morphology assessment without antibodies. (D) JO neuron visualization in live flies by longitudinal imaging (LI) using *iav-GAL4* with engineered fluorescent reporters. (E) Experimental strategy to capture JO adult neurogenesis by MARCM or P-MARCM. Flies are kept at 17°C during development to minimize leaky activation. Two- to five-day-old flies are activated via heat shock and individual antennae are imaged over 4 weeks (w) by fluorescence microscopy. (F-H) Longitudinal imaging of P-MARCM identifies JO neurogenesis (arrowheads) in *Drosophila* antennae (n=19; Fig. 1G) more frequently than MARCM (n=20; Fig. 1F) (****P=0.00014, cumulative probability on binomial distribution; Fig. 1H). Error bars represent s.e.m.

Development (2021) 148, dev187534. doi:10.1242/dev.187534

Identification of JO neurogenesis by P-MARCM

In order to assess the generation of JO neurons in adult *Drosophila*, we used P-MARCM with an *iav-GAL4* line, which drives expression of reporters exclusively in chordotonal neurons (Ishikawa et al., 2017; Kwon et al., 2010) (Fig. S3). Iav (Inactive) is a transient receptor potential (TRP) vanilloid channel expressed exclusively in the cilia of chordotonal neurons, and is essential for mechanotransduction in hearing (Boekhoff-Falk and Eberl, 2014; Gong et al., 2004). Importantly, incorporation of enhanced nuclear-RFP (Barolo et al., 2004) and cytoplasmic GFP (Shearin et al., 2014) reporters in P-MARCM allowed for direct identification of JO neurons by longitudinal live imaging of intact flies (Fig. 1D). We therefore activated P-MARCM *iav-GAL4* in adult flies and conducted single-fly longitudinal imaging over 4 weeks (Fig. 1E). Remarkably, this approach revealed JO neuron generation in P-MARCM flies (47%, n=19 flies) at a significantly higher frequency than transient, regular MARCM (15%, n=20 flies) (Fig. 1F-H).

We then quantified JO neurogenesis by confocal imaging of antennae dissected from P-MARCM *iav-GAL4* flies over 4 weeks (Fig. 2A). Whereas MARCM barely detected neurogenesis, P-MARCM captured increasing amounts of JO neurogenesis over time (Fig. 2B-D). To account for the background levels found in the control group [i.e. non-HS flies at 0 weeks, 4.9±3.9 cells/fly (mean±s.d.), n=16 flies; Fig. S4A], we ran a Gaussian mixture model (Fig. S4B) and determined that any fly in experimental (i.e. HS) groups with ten or more labeled JO neurons can be regarded as undergoing adult neurogenesis with 94% certainty. P-MARCM captured 10-36 JO neurons per fly across time points [20.2±7.3 neurons/fly (mean±s.d.)] (Fig. 2B-D; Fig. S4A). Furthermore, after clustering flies into 'responders' or 'non-responders' (i.e. JO neurogenesis present or absent; Fig. S4B) we observed a significant increase in the number of responders over time (Fig. 2E), occurring in 57% of flies by 4 weeks and 42% across time points. This outcome is consistent with the 47% ratio detected by our longitudinal live imaging approach (Fig. 1H). Taken together, our results identify JO neurogenesis in adult *Drosophila* using complementary *in vivo* longitudinal imaging and confocal microscopy approaches.

Adult-born JO neurons mature and target brain circuitry

We next evaluated the cellular features of newborn JO neurons. Weperformed confocal analysis on antennae and brains of P-MARCM

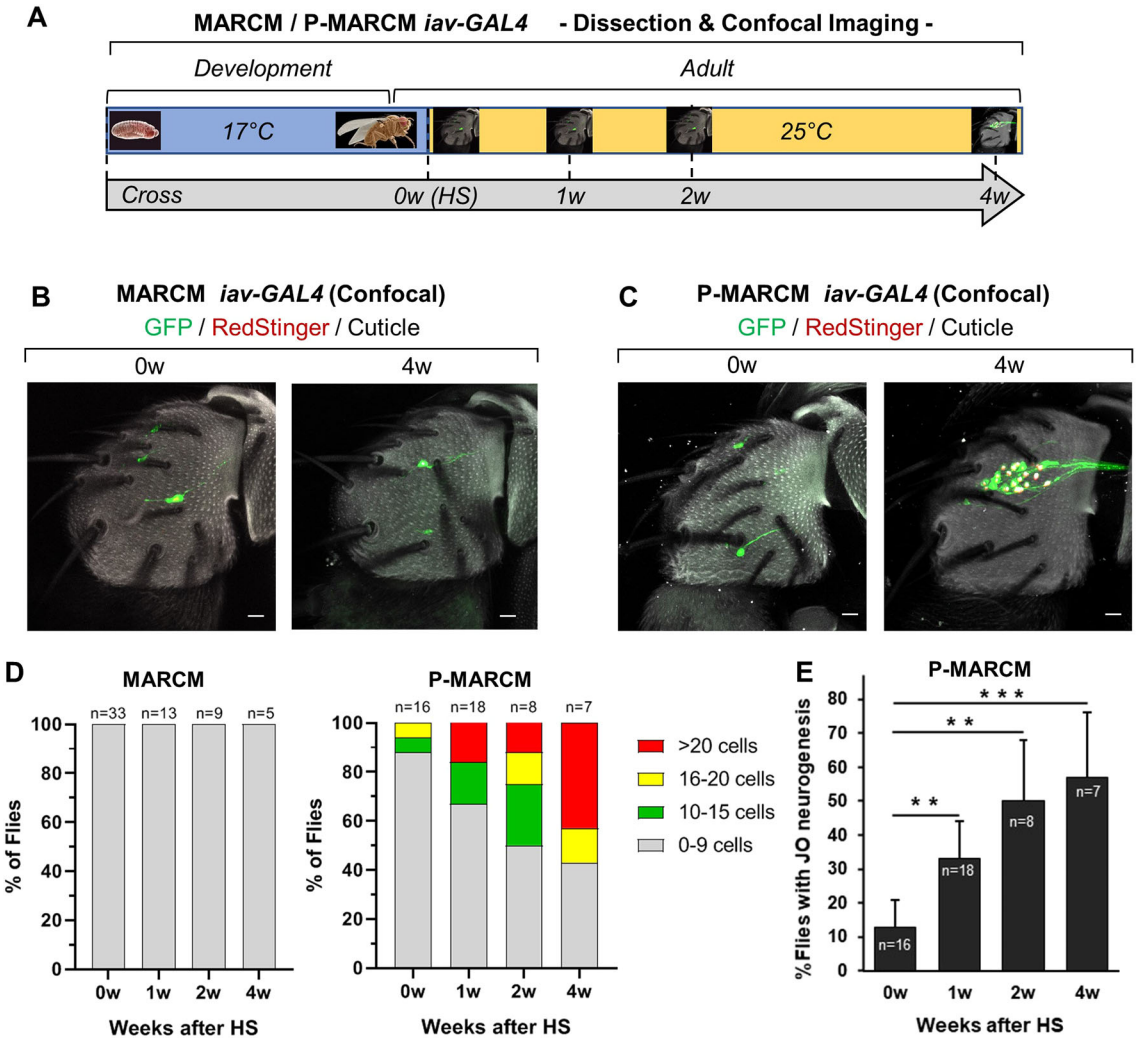

Fig. 2. Quantification of adult JO neurogenesis. (A) Experimental strategy to compute adult JO neurogenesis using MARCM and P-MARCM *iav-GAL4* strategies. Flies (2-5 days old) are heat-shocked (HS) to activate the MARCM or P-MARCM system and antennae are dissected up to 4 weeks (w) later for quantification. (B) Transient MARCM *iav-GAL4* does not capture JO neurogenesis. Scale bars: 10 µm. (C) P-MARCM *iav-GAL4* reveals adult-born JO neurons. Scale bars: 10 µm. (D) The number of adult-born JO neurons increase over time in antennae of P-MARCM, but not MARCM, flies. (E) The number of flies with JO neurogenesis increases over time. **P<0.01; ***P<0.001, cumulative probability on binomial distribution. Error bars represent s.e.m.

Development (2021) 148, dev187534. doi:10.1242/dev.187534

iav-GAL4 flies with JO neurogenesis detected by longitudinal live imaging at 4 weeks (Fig. 3A) (representative images shown for fly in Fig. 1G). At the cellular level, adult-born JO neurons develop cilia and extend axons. Neuronal morphology, including cilia, was visualized in adult-born JO neurons using a cytoplasmic hexameric GFP with enhanced signal (Shearin et al., 2014) without a need for antibodies (Fig. 3B, arrowheads). At the circuit level, new JO neurons project axons to the brain through the antennal mechanosensory and motor center (AMMC) in both auditory (high frequency, Zone A; low frequency, Zone B) and vestibular (backward deflections, Zone E) circuits (Ishikawa and Kamikouchi, 2016; Kamikouchi et al., 2006) (Fig. 3C). These features were consistently found in all cases exhibiting JO neurogenesis. Therefore, these observations strongly suggest new JO neurons can mature and functionally remodel mechanosensory circuitry.

Origin of JO neurons

We next sought to identify a cellular source for adult-born JO neurons. In vertebrates, hair cell regeneration involves transdifferentiation of non-sensory supporting cells (Atkinson et al., 2015; Brignull et al., 2009). Recent studies demonstrate various modes of cell replacement, including proliferation of undifferentiated progenitors, de-differentiation and division of mature cells, and direct mitosis of post-mitotic cell types (Post and Clevers, 2019). We therefore considered three possible sources of adult JO neurons: (1) undifferentiated progenitors maintained from development; (2) non-sensory supporting cells in the scolopidium; and (3) pre-existing JO neurons. To gain insight into possible mechanisms, we observed cells labeled by P-MARCM-iav and MARCM-iav for features of cell division. A detailed analysis of confocal images revealed instances of split DNA on single JO neurons, and pairs of labeled JO with intermingled cilia and axons (Fig. 4A-C), suggesting the possibility of JO self-division (1.3%, n=557 neurons analyzed from 141 antennae).

We next conducted anti-pH3 immunostaining in an attempt to capture mitotic JO neurons. Sparse mitotic figures were found in the optic lobes, a cell-dense region of the brain where P-MARCM also

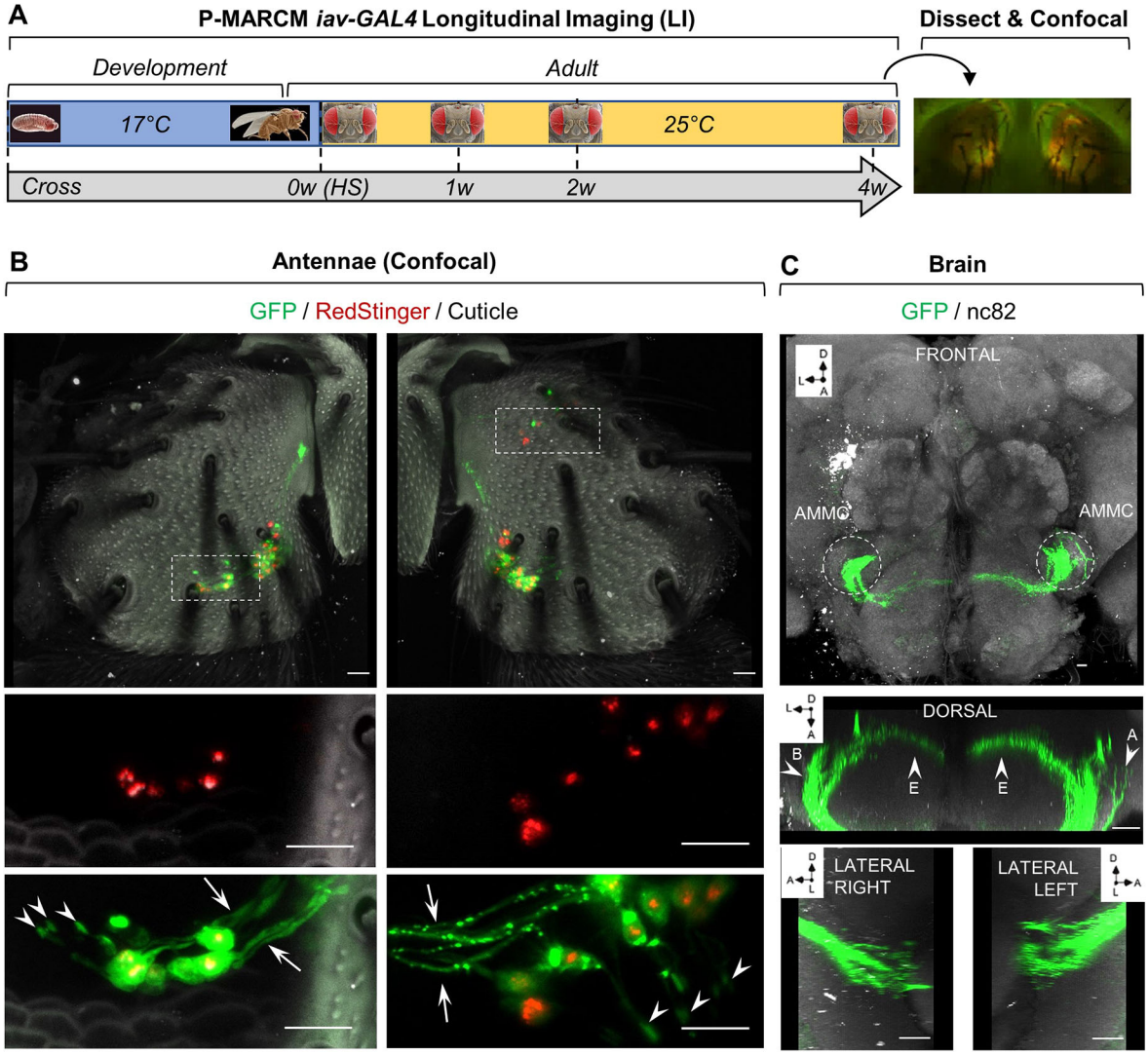

Fig. 3. Adult-born JO neurons acquire mechanosensory features and target brain circuitry. (A) P-MARCM *iav-GAL4* flies with adult JO neurogenesis detected by time lapse imaging (see also Fig. 1E) were dissected for detailed cellular analysis by confocal microscopy (panel here shows adult JO neurogenesis identified by LI from 4 w image in Fig. 1G). w, week. (B) Adult-born JO neurons labeled by the chordotonal neuron-specific iav-GAL4 line develop cilia (arrowheads), and project axons to the central brain (arrows). Scale bars: 10 µm. (C) Axons from adult-born JO neurons target the brain through the antennal mechanosensory and motor center (AMMC) in both auditory [high frequency (arrowhead A) and low frequency (arrowheads B)] and vestibular [backward deflections (arrowheads E)] circuit patterns. A, anterior; D, dorsal; L, lateral; orientations determined according to Ishikawa and Kamikouchi (2016). Scale bars: 10 µm.

Development (2021) 148, dev187534. doi:10.1242/dev.187534

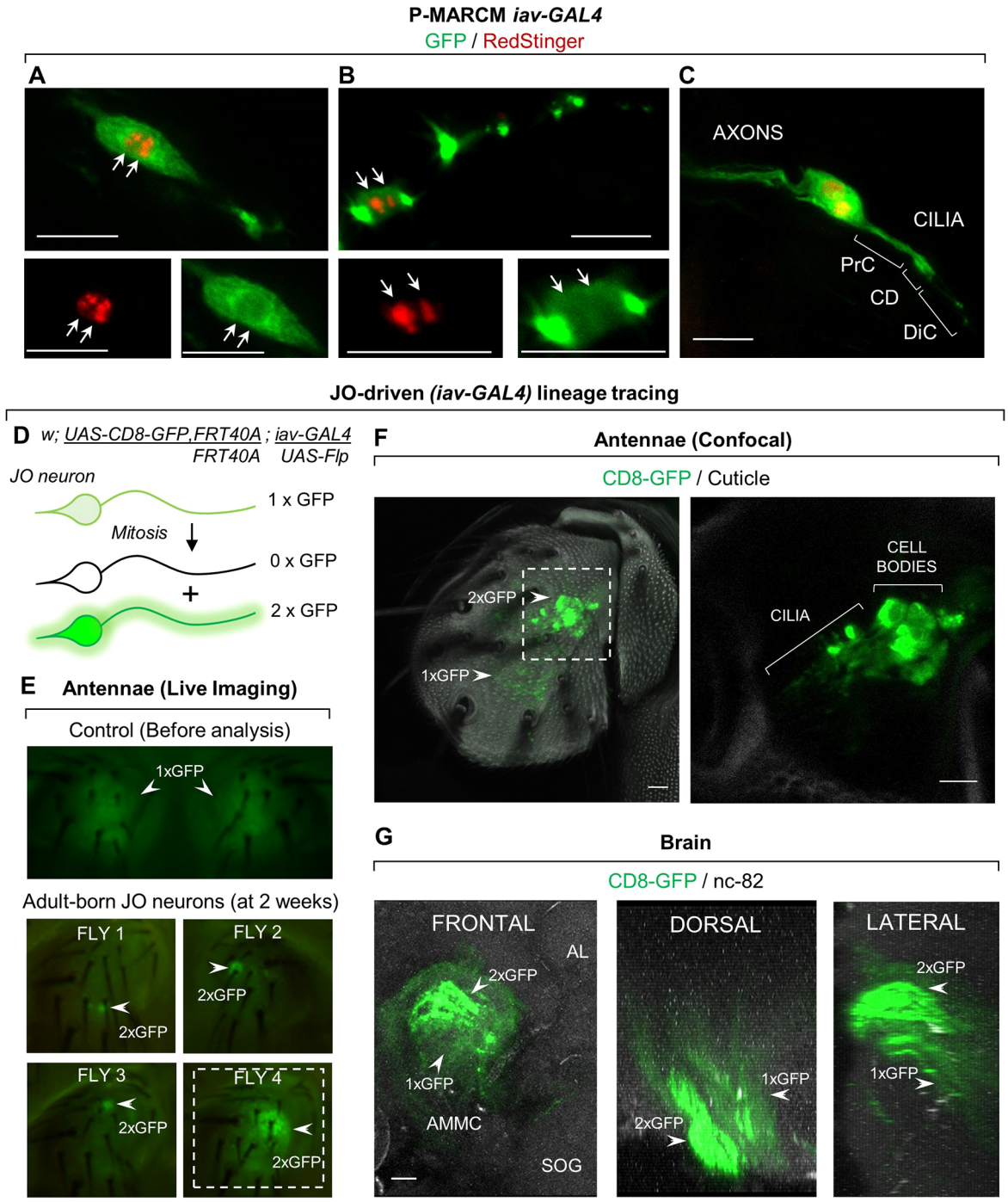

Fig. 4. Adult JO neurons undergo proliferation. (A-C) P-MARCM *iav-GAL4* captures JO neurons with split DNA (A,B) and close proximity (C), suggestive of mitotic activity. CD, ciliary dilation; DiC, distal cilia; PrC, proximal cilia. Scale bars: 10 µm. (D) A lineage tracing system to assess JO proliferation: *iav-GAL4* drives constitutive expression of membrane-tethered GFP and FLP recombinase in JO neurons. Upon mitosis, one JO neuron becomes homozygous for GFP. (E) Clones generated by JO proliferation are detected by fluorescence microscopy in live flies at 2 weeks after ecclosion (arrowheads). Fly 4 is shown in F. (F) A cluster of JO neurons detected in the antennae by confocal microscopy. Right-hand panel is an enlargement of the boxed area to the left. (G) Axons expressing two copies of GFP appear in the brain in an auditory (Zone B) circuit pattern, indicating mature JO neuronal identity via self-division. AL, antennal lobe; AMMC, antennal mechanosensory and motor center; SOG, subesophageal ganglion. Scale bars: 10 µm.

captures proliferation [~40,000 total interneurons/optic lobe (Morante et al., 2011); 9.2±1.0 $pH3^+$ cells/optic lobe (mean± s.e.m.), n=26 optic lobes; Fig. S1D]. However, we did not capture any $pH3^+$ neurons in the JO [data not shown; n=30 antennae; ~500 total JO neurons/antenna (Kamikouchi et al., 2006)]. This observation is consistent with low detection of mitotic figures even in continuously proliferating tissues, such as the adult posterior midgut (approximately two $pH3^+$ cells/gut) (Obata et al., 2018; Ren et al., 2010; Tian and Jiang, 2014).

To overcome detection limitations by immunostaining on low-rate proliferating tissues and to test mitotic activity in JO neurons, we implemented a JO-driven lineage tracing method. Specifically, JO

Development (2021) 148, dev187534. doi:10.1242/dev.187534

neurons constitutively express the recombinase Flippase and a single copy of the UAS-CD8-GFP reporter, distal to an FRT site on the second chromosome. Upon mitosis, one daughter JO neuron becomes homozygous for GFP (2xGFP), clearly distinguishable from the single-copy GFP background (1xGFP) by live imaging (Fig. 4D,E). Although this method does not capture mitotic figures or transitions in phases of the cell cycle, it retrospectively reports on mitotic activity in JO neurons. Remarkably, with this approach we identified a low-level of 2xGFP JO neuron clones at different points over 4 weeks in 20% of the flies analyzed (n=85 flies, 1-11 neurons/antenna) (Fig. 4E,F), pointing to their generation through JO neuron proliferation. In some cases, this approach captured clones at single-neuron resolution (Fig. S5B,C). These cells existed as twin spots (i.e. 2xGFP$^+$ neuron paired with a 0xGFP neuron in a 1xGFP background; Fig. S5D), further supporting the interpretation of JO neuron mitotic division. New JO neurons contained cilia when visualized by a membrane-tethered GFP (Fig. 4F) and 2xGFP JO-axon bundles in the brain, suggestive of JO replication from cell bodies to terminal connections (Fig. 4G). Importantly, JO neuron clones were detected with this method in both males and females (59% males, 41% females, n=17 flies). We ensured that neurons labeled appeared in adult stages by pre-screening every single fly before analysis and removing any 'escapers', labeled by leaky expression of Flippase during development, which appeared at very low rates (2.3%, n=306 flies assessed). In this way, only flies lacking prior recombination were selected for analysis of adult neurogenesis (Fig. 4E).

In order to further determine mitotic activity in JO neurons, we implemented Twin Spot MARCM (Yu et al., 2009) with permanent activity in JO neurons using the *iav-GAL4* line. We called this third mitotic recombination-based lineage tracing approach Perma Twin iav (PT-iav). In this system, differential expression of membrane-tethered GFP and RFP in each hemiclone occurs only in JO neurons arising from JO neuron proliferation events, in an otherwise non-labeled background (Fig. 5A). Remarkably, PT-iav also identified the appearance of JO neuron clones in adult *Drosophila*. GFP$^+$ and RFP$^+$ mitotic clones were apparent when using both *in vivo* longitudinal imaging and confocal microscopy in flies 1-4 weeks old (13% of flies, n=60 flies, 1-17 cells/antennae; Fig. 5B,E). Reproducing earlier findings, we also detected that JO neurons develop cilia and project axons to the brain, suggesting complete JO neuron self-replication (Fig. 5C,D,F,G). Cases of single JO neurons labeled or clones labeled in a single color may indicate that only one daughter neuron survived and kept proliferating upon mitosis. Taken together, our clonal analysis uncovers unexpected mitotic potential in *Drosophila* neurons as a previously unknown mechanism for nervous system regeneration under physiological conditions.

JO cell turnover occurs under physiological conditions

Because cell proliferation in response to cell death in the central brain has been previously demonstrated (Kato et al., 2009), we next asked whether JO regeneration occurs in an additive manner or as a cell turnover mechanism. Immunostaining for cleaved-Caspase3 (Ca3) revealed JO apoptosis at a higher frequency and to a greater extent in posterior neurons [5.8±1.0 Ca3$^+$ neurons/antenna (mean±s.e.m.), 100% antennae, n=33], compared with anterior neurons [1.5±0.25 Ca3$^+$ cells/antenna (mean±s.e.m.), 12% antennae, n=33] (Fig. 6A,C,D). Accordingly, P-MARCM captured JO neurogenesis at a higher frequency and to a greater extent in posterior regions (8.7±2.2 s.e.m. neurons/antenna, 69% antennae, n=16), compared with anterior regions of the antenna [2.4±1.0 neurons/antenna (mean±s.e.m.), 44% antennae, n=16] (Fig. 6B-D). These correlations suggest JO cell turnover. Supporting this finding, the GFP-only JO-specific lineage tracing system also detected JO neuron mitotic recombination clones (i.e. 2xGFP clones) in the vicinity of apoptotic cells (Fig. 6E). Taken together, these results describe cellular plasticity in the mechanosensory system of adult *Drosophila*, pointing to a cell turnover mechanism that could preserve auditory and vestibular functions.

Enhancement of JO neuron regeneration through pharmacological administration

Turnover and regeneration of hair cells proceed to different extents in non-mammalian vertebrates (Bucks et al., 2017; Corwin and Cotanche, 1988; Ryals and Rubel, 1988; Williams and Holder, 2000). Because adult JO neurons turn over under physiological conditions, we hypothesized that JO neurons may also regenerate after different forms of injuries or under environmental perturbation.

Cisplatin is an agent used in cancer therapy with well-known ototoxic side effects: it induces hair cell death in vertebrates (Alam et al., 2000; Ou et al., 2007; Slattery and Warchol, 2010), followed by limited cellular regeneration (Mackenzie and Raible, 2012). In *Drosophila*, administration of cisplatin induces a decrease in negative geotaxis behavior, a function mediated by JO neurons (Podratz et al., 2011). We therefore investigated whether cisplatin-induced injury would increase JO neuron regeneration. We fed flies of the JO-driven GFP lineage tracing system with 50 µg/ml cisplatin over 4 days (Podratz et al., 2011) and examined proliferation over the next 3 days, indicated by the presence of 2xGFP JO neurons (Fig. 7A). Compared with 12% of control flies (n=26) exhibiting mitotic recombination clones with 2.3±1.1 2xGFP new neurons/antenna (mean±s.e.m.) (Fig. 7B,D), we identified an increase in proliferation in 28% of cisplatin-treated flies (n=18), with 4.6±0.9 2xGFP new neurons/antenna (mean±s.e.m.) (Fig. 7C,D). Our results provide evidence for accelerated regenerative capacity of mechanosensory neurons in *Drosophila* following oral administration of this clinical anti-cancer compound.

There is an increasing appreciation of the utility of *Drosophila* as an *in vivo* system for drug screening (Fernández-Hernández et al., 2016; Papanikolopoulou et al., 2019; Su, 2019). To expand our platform's potential for identifying further compounds promoting the self-renewal of JO neurons, we also administered the drug CA-1001 to flies of the Perma Twin-iav system. CA-1001 is a calcium ionophore that we identified in a previous small-molecule screening as a modulator of neurogenesis in the *Drosophila* central nervous system (I.F.-H. and M.A.B., unpublished data). By administering CA-1001 to Perma Twin-*iav* flies in a similar scheme as cisplatin (Fig. 7A), we observed JO neuron regeneration using longitudinal live imaging. GFP$^+$/RFP$^+$ mitotic clones were detected in the antennae of intact adult flies as early as 2 days after the treatment was initiated (Fig. 7E). Confocal imaging revealed that new JO neurons develop cilia and project axons (Fig. 7F) to innervate the brain through the AMMC in both auditory (high frequency, Zone A) and vestibular (backward deflections, Zone E) circuits (Ishikawa and Kamikouchi, 2016) (Fig. 7G; Movie 1 and Fig. S6). Remarkably, proliferation occurred in 14% of the treated flies (n=29 flies), with 8.0±1.8 cells/antenna (mean±s.e.m.), compared with no proliferation detected in the DMSO-treated control flies (n=20 flies) (Fig. 7H). Taken together, our results (1) demonstrate adult JO neurons have the capacity to respond to external stimuli (e.g. drugs) to adjust their proliferation, likely through self-replication, as a mechanism inferred from mitotic recombination clones; and (2) establish a new *in vivo* platform to screen for small molecules that accelerate the regeneration of mechanosensory cells.

Development (2021) 148, dev187534. doi:10.1242/dev.187534

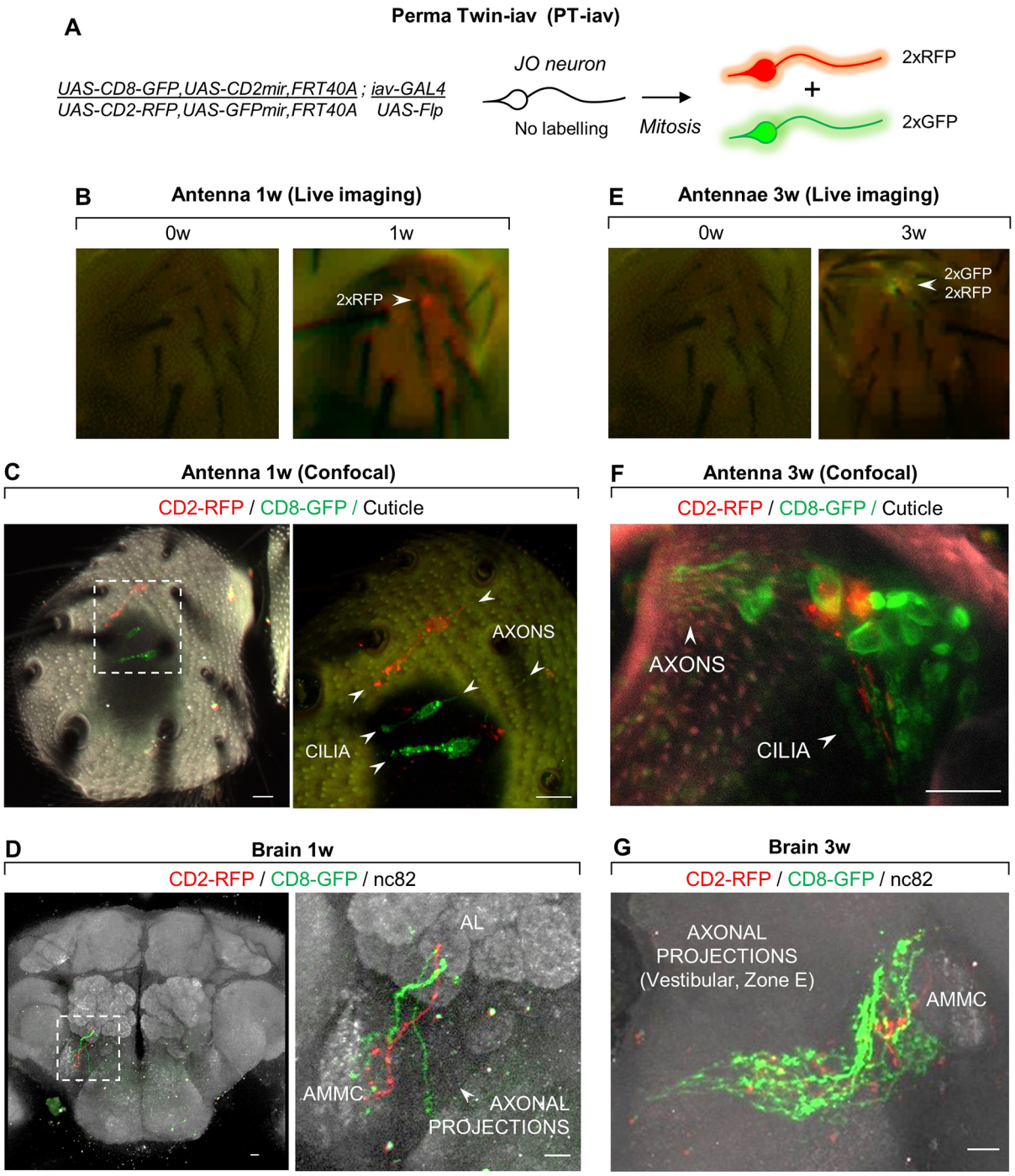

Fig. 5. PT-iav confirms JO neuron proliferation under physiological conditions. (A) In Perma Twin-iav (PT-iav) lineage tracing, GFP and RFP reporters and repressors are differentially segregated upon JO neuron mitosis to label twin progeny hemi-clusters with GFP or RFP. (B) PT-iav reveals JO neuron proliferation in 1-week-old flies by longitudinal live imaging. (C,D) Newborn JO neurons develop cilia and target the brain through the AMMC. Right-hand panel is an enlargement of the boxed area to the left. Arrowheads indicate cilia and axons of adult-born JO neurons. (E) New JO neurons are detected in 3-week-old flies by longitudinal live imaging. (F,G) New neurons develop cilia and send axonal projections to the brain in the vestibular circuit pattern (Zone E). AMMC, antennal mechanosensory and motor center; w, week. Scale bars: 10 µm.

DISCUSSION

There is an urgent need to develop regenerative interventions for lost hair cells. However, the field has been hampered by the lack of *in vivo*, high-throughput platforms to easily assess the functional regeneration of adult sensory cells at the genetic, neural circuitry and behavioral levels. To address this challenge, we developed P-MARCM – a modified lineage tracing system in *Drosophila* for capturing cell type-specific proliferation in adult tissues over time without immunostaining. P-MARCM successfully detected the low rate of neurogenesis and regeneration occurring in adult optic lobes, consistent with previous reports (Fernández-Hernández et al., 2013) (Figs S1 and S2). We leveraged the versatility of P-MARCM to identify adult genesis of JO neurons, the functional counterparts of vertebrate hair cells, by longitudinal imaging of intact flies and

Development (2021) 148, dev187534. doi:10.1242/dev.187534

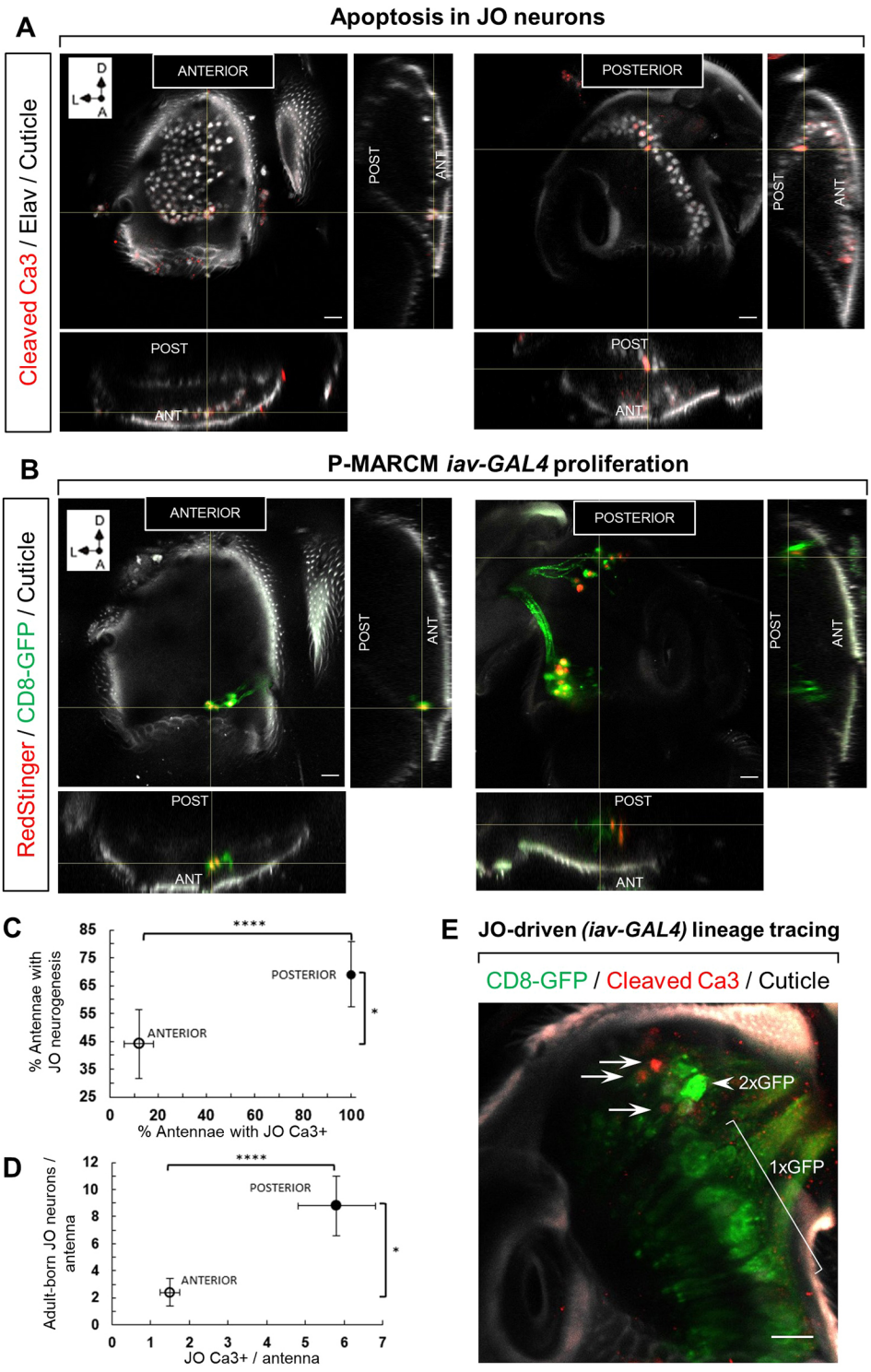

Fig. 6. JO cell turnover occurs under physiological conditions. (A) Apoptotic JO neurons (Cleaved Ca3/Elav) are detected in anterior and posterior regions of the JO array. (B) P-MARCM *iav-GAL4* detects JO neurogenesis in posterior and anterior regions of the JO array. (C) The prevalence of adult JO neurogenesis as detected by P-MARCM (n=16 antennae) correlates with the frequency of apoptosis (n=33 antennae). Error bars represent s.e.m. *P=0.012, ****P<0.0001, cumulative probability on binomial distribution. (D) The number of adult-born JO neurons detected by P-MARCM (n=16 antennae) correlates with the extent of apoptotic JO neurons (n=33 antennae). Error bars represent s.e.m. *P=0.02, ****P<0.0001, Mann–Whitney test. (E) JO neuron production (iav-GAL4, 2xGFP; arrowhead) occurs adjacent to apoptotic JO neurons (arrows). Non-dividing JO neurons contain a single copy of GFP (iav-GAL4, 1xGFP lineage tracing. A, anterior; D, dorsal; L, lateral. Scale bars: 10 µm.

confocal microscopy. However, the P-MARCM version reported here is not without limitations. For example, use of FRT recombination sites on the X chromosome currently restricts its application to analysis of cell proliferation in females. Also, long-term time-lapse recording is not feasible on this platform without compromising *Drosophila* viability. Nonetheless, this platform enabled longitudinal observation of new cell addition to external organs *in vivo* at discrete time points in single flies. Furthermore, the incorporation of an additional *UAS*-construct permits genetic manipulation of adult-born cells to assess their functional contributions. For example, future experiments could assess the contribution of JO neurons to auditory and vestibular function by applying existing behavioral protocols (Inagaki et al., 2010; Kamikouchi et al., 2009; Vaughan et al., 2014). Indeed, our results suggest that new JO neurons have the potential to functionally modify mechanosensory circuitry, as they develop sensory cilia, and target appropriate auditory and vestibular circuits. This system will also enable research on mechanisms driving synapse formation between new and pre-existing neurons.

A central question in regenerative medicine is identifying a cell of origin that initiates tissue turnover. Cell replacement in different

Development (2021) 148, dev187534. doi:10.1242/dev.187534

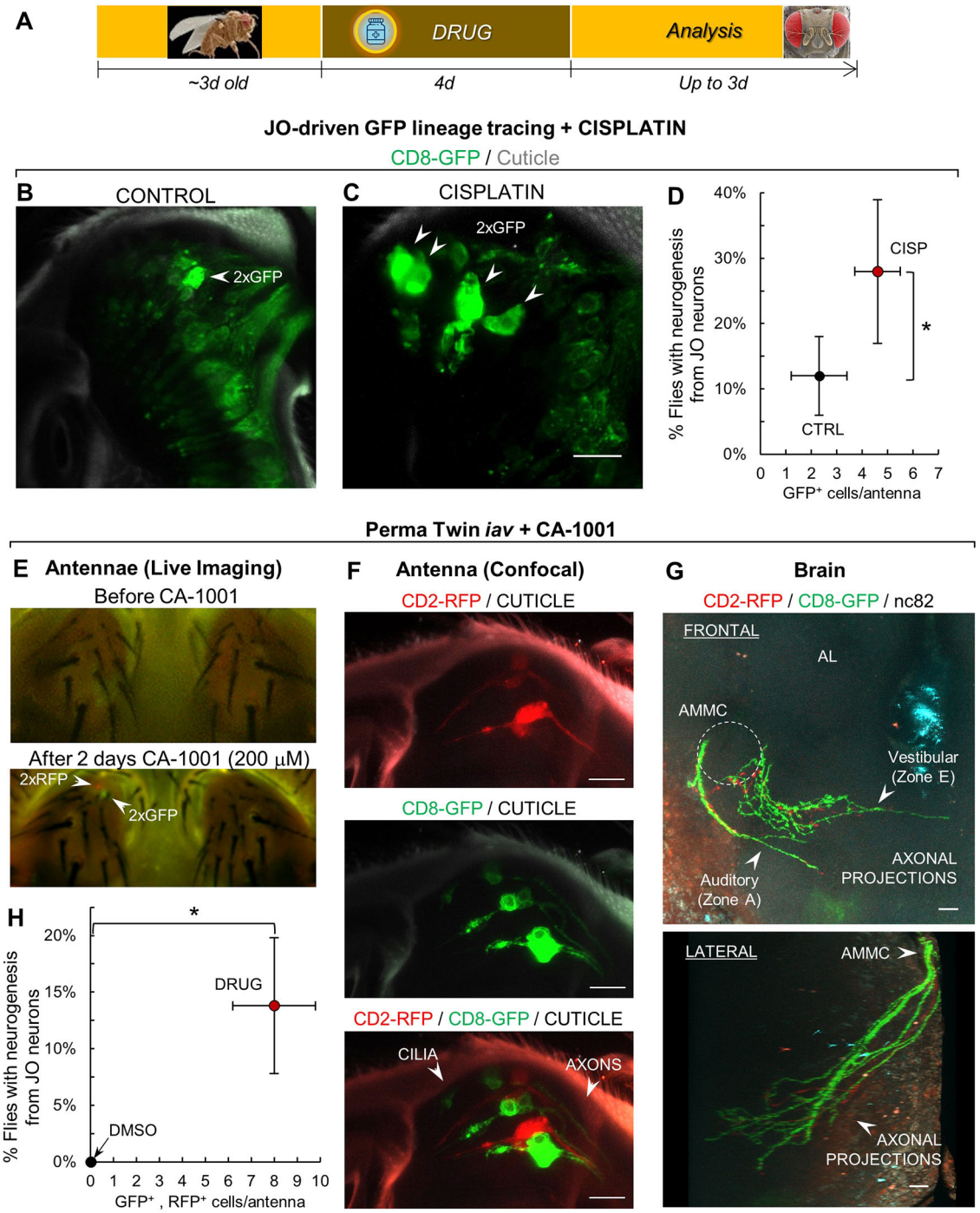

Fig. 7. Enhancement of JO neuron regeneration through pharmacological administration. (A) Experimental timeline for pharmacological administration. Flies (2-3 days old) were fed over 4 days with control DMSO or drug-supplemented food. JO neuron proliferation was assessed up to 3 days later. (B,C) 2xGFP cells from JO-driven lineage tracing reveals JO neurogenesis in control (B) and cisplatin-treated (C) fly antennae. (D) Cisplatin administration increases the frequency and amount of JO neuron production [n=26 control (CTRL) flies; n=18 cisplatin flies]. *P=0.02, cumulative probability of bionomial distribution. Error bars represent s.e.m. (E) The calcium ionophore CA-1001 triggers proliferation of JO neurons, as detected in live flies by fluorescent microscopy. New neurons are marked by the appearance of GFP$^+$ and RFP$^+$ hemiclusters (twins) using the PT-iav system. (F) New JO neurons develop cilia and send axons to the brain. Top: RFP hemicluster; middle: GFP hemicluster; bottom: merged cluster. (G) CA-1001-induced JO neurons display auditory (zone A) and vestibular (zone E) circuit patterns. Axonal projections analyzed according to Ishikawa and Kamikouchi (2016). AL, antennal lobe; AMMC, antennal mechanosensory and motor center. (H) CA-1001 administration increases the frequency and amount of JO neuron production [n=20 control (DMSO) flies; n=29 CA-1001 flies]. *P=0.02 by one-sample t-test. Error bars represent s.e.m. Scale bars: 10 µm.

tissues involves diverse mechanisms and cellular sources, including proliferation of undifferentiated progenitors, de-differentiation and division of mature cells, and direct mitosis of post-mitotic cells (Post and Clevers, 2019). Analysis of P-MARCM images prompted us to hypothesize that JO neurons could self-divide and remain in the tissue. We performed immunostaining for the mitotic marker pH3 on JO neurons to provide direct evidence of their proliferation, but were unable to capture this very brief state on the samples analyzed.

Development (2021) 148, dev187534. doi:10.1242/dev.187534

We instead implemented two JO-specific lineage tracing methods that differentially label only JO neurons produced through inferred self-division events in a cumulative way, retrospectively reporting on cell proliferation. Surprisingly, these methods revealed mitotic recombination clones imaged on intact live flies. Therefore, even though proliferation in JO neurons is yet to be demonstrated using mitotic markers, these results suggest an unexpected proliferative capacity of JO neurons and confirmed the JO neurogenesis detected by P-MARCM. Other proliferative cell types have been identified in the adult *Drosophila* nervous system, including Repo^{+} glial cells (Kato et al., 2009) and Repo^{-}/miR31a^{+} progenitors in the central brain (Foo et al., 2017), as well as undifferentiated Dpn^{+} cells in the central brain and the optic lobes (Fernández-Hernández et al., 2013; Li et al., 2020). Altogether, these reports exemplify the diversity of cellular sources used by different organs or regions in a tissue in order to undergo cell renewal. Niche restrictions on progenitor cells and the ease with which progeny can be incorporated into the pre-existing tissue may determine which mechanisms are utilized. In the optic lobes, for example, the wider surface of this region could facilitate the accommodation of an undifferentiated progenitor to proliferate and eventually incorporate its progeny. As for the JO, the neuron self-renewal inferred from the mitotic recombination systems might have evolved as a regenerative mechanism because (1) JO neurons are enclosed by three distinct supporting cells in the scolopidium, making it challenging to incorporate external JO neurons from an external progenitor; (2) each scolopidium contains two or three JO neurons, a potential back-up mechanism to promptly replace lost neurons without compromising other scolopidial cell types; and (3) self-division would facilitate proper cilia- and axon-targeting for optimal function in new JO. An interesting question related to this is whether a differential JO regenerative response exists upon selective ablation of a single versus multiple JO neurons in a scolopidium. Overall, it will be compelling to further investigate JO neuron self-division and its underlying cellular and molecular mechanisms.

At the same time, our Perma Twin iav results do not exclude the presence of an undifferentiated progenitor in the antennae as an additional cell of origin for new JO neurons, and potentially for other cell types in the scolopidium. Indeed, P-MARCM iav (which becomes ubiquitously activated upon heat shock) captured higher proliferation rates (45% of the flies) than Perma Twin-iav (13% of the flies), suggesting additional JO cell sources. Alternatively, the observed differences could simply reflect recombination efficiencies between our methods. Taken together, three independent lineage tracing methods converge to demonstrate the generation of mechanosensory cells in the antennae of adult *Drosophila*, and to suggest the self-renewal of JO neurons as an unexpected mechanism of sensory cell regeneration. Furthermore, these results raise the possibility that self-renewal of neurons might occur in other regions of the adult nervous system, as an adaptive regenerative mechanism to preserve tissue homeostasis and function.

Recent efforts have established mammalian *in vitro* platforms for drug screening to promote hair cell renewal (Costa et al., 2015; Koehler et al., 2013, 2017; Landegger et al., 2017). Although useful, these platforms lack physiological environmental and systemic cues, such as those controlling tissue interactions, as well as drug metabolism and availability. In our case, the low levels of apparent JO self-division reported by the lineage tracing systems and the sensitivity that allows newborn neurons to be identified by longitudinal live imaging of individual flies provides an *in vivo* scalable platform to screen for small molecules with translational relevance that enhance JO regeneration (Fernández-Hernández et al., 2016). Indeed, we provide a proof of principle of enhanced JO neuron regeneration upon the oral administration of cisplatin, a common ototoxic drug, and CA-1001, a calcium modulator. Cisplatin is known to kill hair cells in vertebrates, which regenerate afterwards up to a limited extent in the zebrafish lateral line (Mackenzie and Raible, 2012). Our results suggest a similar compensatory proliferation triggered in the JO neurons following cisplatin administration. CA-1001 is a calcium ionophore which facilitates the transport of Ca^{2+} across the plasma membrane. Here, Ca^{2+} might play a direct role in the generation of JO neurons, as calcium signaling is a known regulator of cell proliferation, the expression of genes involved in cell growth, and the early steps of neurogenesis (Leclerc et al., 2012; Pinto et al., 2015; Resende et al., 2013). Although elucidation of the molecular mechanisms driving regeneration of JO neurons is pending, for these as well as for other selected drug hits, the transcriptomic and epigenetic changes in JO neurons can be assessed as they occur *in vivo*, by available genetically encoded tools (Marshall and Brand, 2017; Marshall et al., 2016; Southall et al., 2013). Furthermore, the functional contribution of regenerated JO can be readily assessed by established behavioral protocols (Kamikouchi et al., 2009; Sun et al., 2009; Vaughan et al., 2014). In summary, the new *Drosophila* platform presented here represents a promising approach for identifying modifiers of neuronal regeneration, their mechanisms of action and their functional consequences at both the circuitry and behavioral levels.

MATERIALS AND METHODS

Fly lines and experimental conditions

P-MARCM-iav and MARCM-iav experiments

Female virgins of genotype *hs-Flp, tub-GAL80, neoFRT19A; hs-FlpD5, 20UAS-6GFPmyr,UAS-RedStinger/CyO; iav-GAL4* were crossed to males of genotype *tub FRT STOP FRT lexA,neoFRT19A;+; 8lexAOp-Flp/TM6B*. The cross was set and kept at 17°C during development to minimize spontaneous *hs-Flp* activation. For P-MARCM, we picked 2- to 5-day-old female virgins with final genotype *hs-Flp,tub-GAL80,neoFRT19A/tub FRT STOP FRT lexA,neoFRT19A; hs-FlpD5, 20UAS-6GFPmyr, UAS-RedStinger/+; iav-GAL4/8lexAOp-Flp*. For MARCM, females of the same age and genotype, but carrying a *TM6B* balancer chromosome instead of *8lexAOp-Flp* were picked. *hs-FlpD5* (Nern et al., 2011) was inserted to maximize FLP induction and recombination. Every single fly of these genotypes was then pre-screened under an epi-fluorescent scope to ensure only those with minimum to no background labeling were used for proliferation analysis. Selected flies were then pooled, and control ones randomly picked for dissection corresponding to the '0 w' time point. Remaining flies were allocated for activation by heat shock and dissection at later time points. In order to maximize the number of cells with the system activated, flies were heat-shocked at 38°C (Ohlstein and Spradling, 2006) for 30 min twice on the same day, ∼2 h apart.

P-MARCM-nsyb experiments (Fig. S1)

Here, flies of final genotype *hs-Flp, tub-GAL80, neoFRT19A/tub FRT STOP FRT lexA, neoFRT19A; 20UAS-6GFPmyr, UAS-RedStinger/+; nsyb-GAL4/8lexAOp-Flp* were used. Because preliminary assessment of background labeling in the brain is not possible without dissection, only one copy of regular *hs-Flp* was included to minimize leaky expression. Flies were blindly assigned to the control group for dissection and to the experimental group for heat shock at 38°C for 45 min twice on the same day, ∼2 h apart, and dissected 3 weeks later.

JO-driven (iav-GAL4) lineage tracing system

Female virgins of genotype *w; UAS-CD8-GFP, UAS-CD2mir, FRT40A; 20UAS-FlpD5* were crossed to males of genotype *w; tubQS, FRT40A; iav-GAL4*. We selected males and females, 2-5 days old, with the final genotype *w; UAS-CD8-GFP,UAS-CD2mir, FRT40A/tub-QS,FRT40A; 20UAS-FlpD5/*

Development (2021) 148, dev187534. doi:10.1242/dev.187534

iav-GAL4. These flies were then screened individually by fluorescent microscopy to remove those with background labeling. Selected flies were tracked weekly over 4 weeks, and those with JO neurogenesis were live-imaged by fluorescent microscopy (see below) and harvested for confocal imaging, as described below.

PT-iav lineage tracing system

Female virgins of genotype *w; UAS-CD8-GFP, UAS-CD2mir, FRT40A; 20UAS-FlpD5* were crossed to males of genotype *w; UAS-CD2-RFP, UAS-GFPmir,FRT40A; iav-GAL4*. Males and females, 2-5 days old, with the final genotype *w; UAS-CD8-GFP,UAS-CD2mir, FRT40A/UAS-CD2-RFP, UAS-GFPmir, FRT40A; 20UAS-FlpD5/iav-GAL4* were used. These flies were screened individually by fluorescent microscopy to remove those with background labeling. Selected flies were either tracked weekly between 1 and 4 weeks in physiological conditions or up to 3 days after drug administration for JO neurons regeneration.

Drug treatment

Cisplatin (Sigma-Aldrich, 479306-1) was freshly prepared dissolved at 50 µg/ml (final concentration) in ddH_2O. As a control, ddH_2O was used. CA-1001 (Cayman Chemical, 17407) was prepared as a 10 mM stock solution in pure DMSO and stored at −20C, for further dilution to 100 µM or 200 µM for experimental use. As control, 1% or 2% DMSO was used. About 200 mg of instant fly food in powder form was reconstituted with 1 ml of the corresponding drug or control solution in an empty plastic vial, where fewer than ten flies were placed for treatment over 2 days, when they were transferred to another vial with fresh drug-containing food for an additional 2 days. After a total of 4 days treatment, flies were transferred to vials with regular food for tracking JO neurogenesis up to 3 days later. Those with JO neurogenesis were live-imaged by fluorescent microscopy (see below) and harvested for confocal imaging as described below.

Dissection, immunostaining and confocal imaging

Antennae were dissected, attached to their corresponding brains in chilled Schneider's medium, and then fixed in 3.7% formaldehyde solution for 20 min. They were then washed with 1% Triton X-100 in PBS solution for 10-20 min, followed by a final wash in 1×PBS before incubation with primary antibodies overnight at 4°C (two nights for nc-82 antibody), followed by incubation with secondary antibody for 4 h at room temperature or overnight at 4°C. For staining of neurons and caspase, the third segment of antennae was removed before fixation, to facilitate antibody penetration to JO neurons. Primary antibodies were: mouse anti-nc82 [1:10, DSHB deposited by E. Buchner (Wagh et al., 2006)], rat anti-Elav [1:100, DSHB, deposited by Gerald M. Rubin (O'Neill et al., 1994)], rabbit anti-cleaved Caspase3 (1:200, Cell Signaling Technology, 9664T); rabbit anti-pH3 (1:100, Cell Signaling Technology, 9701). Secondary antibodies (Jackson ImmunoResearch Laboratories) were: anti-mouse Alexa Fluor 647 antibody (1:100, 715-606-151), anti-rat Alexa Fluor 647 (1:100, 712-606-153), anti-rabbit Cy3 (1:200, 711-166-152) and anti-rabbit Alexa Fluor 488 (1:200711-546-152). No antibodies were used for GFP, RFP or RedStinger fluorescent proteins. Antennae and brains were mounted in Vectashield media with DAPI (Vector Laboratories). For mounting, we used double-side sticker spacers (EMS, 70327-9S) to preserve morphology as much as possible. We used one spacer for antennae and two for matching brains. Images were acquired on a Zeiss LSM 700 confocal microscope at either 1.2 µm spacing with 20× objective or 0.6 µm spacing with 40× objective. Images shown represent maximum intensity projections of relevant planes or 3D projections.

Longitudinal imaging of live flies

For Fig. 1 results, MARCM-iav and P-MARCM-iav flies were kept isolated over the analysis period in individual 1.5 ml centrifuge tubes containing regular fly food and with a hole in the cap to allow oxygen exchange while preventing flies from escaping. Images were acquired once weekly from the same individuals using the settings listed below. Antennae from flies shown in Fig. 3 were processed for confocal imaging at the end of the analysis period. For the JO-specific lineage tracing systems, every single fly was pre-screened under fluorescent scope (Zeiss V16) to retain only those with no background labeling and then were maintained together in a regular vial with food. Every single fly was then screened under the fluorescent scope at later time points (weekly for physiological conditions, up to 3 days for drug treatments) and those in which JO neurogenesis was detected were harvested for confocal imaging.

Flies were anesthetized on a CO_2 pad for imaging under a Zeiss V16 epi-fluorescent scope with a 5.6 Mp monochrome camera. These acquisition settings were selected to image P-MARCM flies in order to preserve viability after imaging over time: 50% power lamp, PlanApo 1× objective, 85% aperture, 160× total magnification, 5×5 camera binning, 90 ms exposure time for GFP and RFP channels, and, on average, a ∼65 µm *z*-stack with 4 µm increments. For JO-lineage tracing 4×4 camera binning was selected. Maximum intensity projections were generated for display.

Gaussian mixture model method

Labeled neurons were counted in the JO of each fly, from all time points. Assuming JO from any time point fell into either 'responder' or 'non-responder' categories, we fitted a Gaussian mixture model with two mixture components using the mclust package (Scrucca et al., 2016) with default parameters. The model found that any fly with nine or fewer neurons was in the non-responder category (i.e. comparable to system background levels), which accounted for 63% of all observations, and any fly with ten or more neurons was a responder (i.e. above background levels), accounting for the remaining 37% of all observations.

Statistical analysis

Plots and statistical analysis were done using GraphPad Prism and Microsoft Excel with data from at least three replicate groups (two groups for cisplatin tests), based on Student's *t*-test or the cumulative probability of binomial distributions. s.e.m. on experiments with binary outcomes was calculated as $\sqrt{p(1-p)/n}$, where p is the frequency of JO neurogenesis in the analyzed group, and n the number of flies considered. In the quantification of JO neurons labeled with MARCM and P-MARCM systems (Fig. S4), any value above 2.5 s.d. from the mean was considered an outlier. This yielded for MARCM: 1/33 outlier at 0 w (28 JO neurons labeled); and for P-MARCM: 1/17 outlier in the 0 w group (45 JO neurons labeled) and 1/19 outlier in the 1 w group (42 JO neurons labeled), which were excluded from analysis.

Acknowledgements

We thank members of the Bonaguidi lab for support, especially Maxwell Bay for assistance with the Gaussian model and statistical analysis, and Eric Hu for technical assistance with maintenance of fly lines; Dr Neil Segil (USC) for directing our attention to the auditory system of the fly and for insightful discussions on this project; Dr Matthias Landgraf (University of Cambridge) for kindly providing *tub>STOP>lexA* flies; Cristy Lytal for editing the manuscript; Bloomington *Drosophila* Stock Center (National Institutes of Health P40OD018537) for other lines used in this study; and Developmental Studies Hybridoma Bank, created by the National Institute of Child Health and Human Development of the National Institutes of Health for nc-82 and Elav antibodies.

Competing interests

The authors declare no competing or financial interests.

Author contributions

Conceptualization: I.F.-H., M.A.B.; Methodology: I.F.-H.; Validation: I.F.-H.; Formal analysis: I.F.-H.; Investigation: I.F.-H., E.B.M.; Resources: M.A.B.; Data curation: I.F.-H., M.A.B.; Writing - original draft: I.F.-H.; Writing - review & editing: M.A.B.; Supervision: M.A.B.; Funding acquisition: I.F.-H., M.A.B.

Funding

This work was supported by a USC-CONACYT (Consejo Nacional de Ciencia y Tecnología) Postdoctoral Scholars Program Fellowship and a USC Provost's Postdoctoral Scholar Research Grant to I.F.-H.; USC Provost Undergraduate Research Fellowship to E.B.M.; and grants from the National Institutes of Health (R00NS089013, R56AG064077), the L. K. Whittier Foundation, the Donald E. and Delia B. Baxter Foundation, and Eli and Edythe Broad Foundation to M.A.B. Deposited in PMC for release after 12 months.

Supplementary information

Supplementary information available online at
https://dev.biologists.org/lookup/doi/10.1242/dev.187534.supplemental

References

Alam, S. A., Ikeda, K., Oshima, T., Suzuki, M., Kawase, T., Kikuchi, T. and Takasaka, T. (2000). Cisplatin-induced apoptotic cell death in Mongolian gerbil cochlea. *Hear. Res.* **141**, 28-38. doi:10.1016/S0378-5955(99)00211-7

Albert, J. T. and Göpfert, M. C. (2015). Hearing in *Drosophila*. *Curr. Opin. Neurobiol.* **34**, 79-85. doi:10.1016/j.conb.2015.02.001

Atkinson, P. J., Huarcaya Najarro, E., Sayyid, Z. N. and Cheng, A. G. (2015). Sensory hair cell development and regeneration: similarities and differences. *Development* **142**, 1561-1571. doi:10.1242/dev.114926

Barolo, S., Castro, B. and Posakony, J. W. (2004). New *Drosophila* transgenic reporters: insulated P-element vectors expressing fast-maturing RFP. *BioTechniques* **36**, 436-40, 442. doi:10.2144/04363ST03

Boekhoff-Falk, G. (2005). Hearing in *Drosophila*: development of Johnston's organ and emerging parallels to vertebrate ear development. *Dev. Dyn.* **232**, 550-558. doi:10.1002/dvdy.20207

Boekhoff-Falk, G. and Eberl, D. F. (2014). The *Drosophila* auditory system. *Wiley Interdiscip. Rev. Dev. Biol.* **3**, 179-191. doi:10.1002/wdev.128

Bramhall, N. F., Shi, F., Arnold, K., Hochedlinger, K. and Edge, A. S. B. (2014). Lgr5-positive supporting cells generate new hair cells in the postnatal cochlea. *Stem Cell Rep.* **2**, 311-322. doi:10.1016/j.stemcr.2014.01.008

Brignull, H. R., Raible, D. W. and Stone, J. S. (2009). Feathers and fins: non-mammalian models for hair cell regeneration. *Brain Res.* **1277**, 12-23. doi:10.1016/j.brainres.2009.02.028

Bucks, S. A., Cox, B. C., Vlosich, B. A., Manning, J. P., Nguyen, T. B. and Stone, J. S. (2017). Supporting cells remove and replace sensory receptor hair cells in a balance organ of adult mice. *eLife* **6**, e18128. doi:10.7554/eLife.18128

Corwin, J. T. and Cotanche, D. A. (1988). Regeneration of sensory hair cells after acoustic trauma. *Science* **240**, 1772-1774. doi:10.1126/science.3381100

Costa, A., Sanchez-Guardado, L., Juniat, S., Gale, J. E., Daudet, N. and Henrique, D. (2015). Generation of sensory hair cells by genetic programming with a combination of transcription factors. *Development* **142**, 1948-1959. doi:10.1242/dev.119149

Cox, B. C., Chai, R., Lenoir, A., Liu, Z., Zhang, L., Nguyen, D.-H., Chalasani, K., Steigelman, K. A., Fang, J., Rubel, E. W. et al. (2014). Spontaneous hair cell regeneration in the neonatal mouse cochlea in vivo. *Development* **141**, 1599-1599. doi:10.1242/dev.109421

Eberl, D. F. and Boekhoff-Falk, G. (2007). Development of Johnston's organ in *Drosophila*. *Int. J. Dev. Biol.* **51**, 679-687. doi:10.1387/ijdb.072364de

Fernández-Hernández, I., Rhiner, C. and Moreno, E. (2013). Adult neurogenesis in *Drosophila*. *Cell Rep.* **3**, 1857-1865. doi:10.1016/j.celrep.2013.05.034

Fernández-Hernández, I., Scheenaard, E., Pollarolo, G. and Gonzalez, C. (2016). The translational relevance of *Drosophila* in drug discovery. *EMBO Rep.* **17**, 471-472. doi:10.15252/embr.201642080

Foo, L. C., Song, S. and Cohen, S. M. (2017). miR-31 mutants reveal continuous glial homeostasis in the adult *Drosophila* brain. *EMBO J.* **36**, 1215-1226. doi:10.15252/embj.201695861

Forge, A., Li, L., Corwin, J. T. and Nevill, G. (1993). Ultrastructural evidence for hair cell regeneration in the mammalian inner ear. *Science* **259**, 1616-1619. doi:10.1126/science.8456284

Geleoc, G. S. G. and Holt, J. R. (2014). Sound strategies for hearing restoration. *Science* **344**, 1241062-1241062. doi:10.1126/science.1241062

Golub, J. S., Tong, L., Ngyuen, T. B., Hume, C. R., Palmiter, R. D., Rubel, E. W. and Stone, J. S. (2012). Hair cell replacement in adult mouse utricles after targeted ablation of hair cells with diphtheria toxin. *J. Neurosci.* **32**, 15093-15105. doi:10.1523/JNEUROSCI.1709-12.2012

Gong, Z., Son, W., Chung, Y. D., Kim, J., Shin, D. W., McClung, C. A., Lee, Y., Lee, H. W., Chang, D.-J., Kaang, B.-K. et al. (2004). Two interdependent TRPV channel subunits, inactive and Nanchung, mediate hearing in *Drosophila*. *J. Neurosci.* **24**, 9059-9066. doi:10.1523/JNEUROSCI.1645-04.2004

Inagaki, H. K., Kamikouchi, A. and Ito, K. (2010). Methods for quantifying simple gravity sensing in *Drosophila* melanogaster. *Nat. Protoc.* **5**, 20-25. doi:10.1038/nprot.2009.196

Ishikawa, Y. and Kamikouchi, A. (2016). Auditory system of fruit flies. *Hear. Res.* **338**, 1-8. doi:10.1016/j.heares.2015.10.017

Ishikawa, Y., Okamoto, N., Nakamura, M., Kim, H. and Kamikouchi, A. (2017). Anatomic and physiologic heterogeneity of subgroup-A auditory sensory neurons in fruit flies. *Front. Neural Circuits* **11**, 46. doi:10.3389/fncir.2017.00046

Kamikouchi, A., Shimada, T. and Ito, K. (2006). Comprehensive classification of the auditory sensory projections in the brain of the fruit fly *Drosophila* melanogaster. *J. Comp. Neurol.* **499**, 317-356. doi:10.1002/cne.21075

Kamikouchi, A., Inagaki, H. K., Effertz, T., Hendrich, O., Fiala, A., Göpfert, M. C. and Ito, K. (2009). The neural basis of *Drosophila* gravity-sensing and hearing. *Nature* **458**, 165-171. doi:10.1038/nature07810

Kato, K., Awasaki, T. and Ito, K. (2009). Neuronal programmed cell death induces glial cell division in the adult *Drosophila* brain. *Development* **136**, 51-59. doi:10.1242/dev.023366

Kawamoto, K., Izumikawa, M., Beyer, L. A., Atkin, G. M. and Raphael, Y. (2009). Spontaneous hair cell regeneration in the mouse utricle following gentamicin ototoxicity. *Hear. Res.* **247**, 17-26. doi:10.1016/j.heares.2008.08.010

Kelley, M. W., Talreja, D. R. and Corwin, J. T. (1995). Replacement of hair cells after laser microbeam irradiation in cultured organs of corti from embryonic and neonatal mice. *J. Neurosci.* **15**, 3013-3026. doi:10.1523/JNEUROSCI.15-04-03013.1995

Kniss, J. S., Jiang, L. and Piotrowski, T. (2016). Insights into sensory hair cell regeneration from the zebrafish lateral line. *Curr. Opin. Genet. Dev.* **40**, 32-40. doi:10.1016/j.gde.2016.05.012

Koehler, K. R., Mikosz, A. M., Molosh, A. I., Patel, D. and Hashino, E. (2013). Generation of inner ear sensory epithelia from pluripotent stem cells in 3D culture. *Nature* **500**, 217-221. doi:10.1038/nature12298

Koehler, K. R., Nie, J., Longworth-Mills, E., Liu, X.-P., Lee, J., Holt, J. R. and Hashino, E. (2017). Generation of inner ear organoids containing functional hair cells from human pluripotent stem cells. *Nat. Biotechnol.* **35**, 583-589. doi:10.1038/nbt.3840

Kwon, Y., Shen, W. L., Shim, H.-S. and Montell, C. (2010). Fine thermotactic discrimination between the optimal and slightly cooler temperatures via a TRPV channel in chordotonal neurons. *J. Neurosci.* **30**, 10465-10471. doi:10.1523/JNEUROSCI.1631-10.2010

Lai, J. S.-Y., Lo, S.-J., Dickson, B. J. and Chiang, A.-S. (2012). Auditory circuit in the *Drosophila* brain. *Proc. Natl. Acad. Sci. USA* **109**, 2607-2612. doi:10.1073/pnas.1117307109

Landegger, L. D., Dilwali, S. and Stankovic, K. M. (2017). Neonatal murine cochlear explant technique as an in vitro screening tool in hearing research. *J. Vis. Exp.* **124**, 55704. doi:10.3791/55704

Leclerc, C., Néant, I. and Moreau, M. (2012). The calcium: an early signal that initiates the formation of the nervous system during embryogenesis. *Front. Mol. Neurosci.* **5**, 64. doi:10.3389/fnmol.2012.00064

Lee, T. and Luo, L. (1999). Mosaic analysis with a repressible cell marker for studies of gene function in neuronal morphogenesis. *Neuron* **22**, 451-461. doi:10.1016/S0896-6273(00)80701-1

Lee, P.-T., Zirin, J., Kanca, O., Lin, W.-W., Schulze, K. L., Li-Kroeger, D., Tao, R., Devereaux, C., Hu, Y., Chung, V. et al. (2018). A gene-specific T2A-GAL4 library for *Drosophila*. *eLife* **7**, e35574. doi:10.7554/eLife.35574

Li, T., Bellen, H. J. and Groves, A. K. (2018). Using *Drosophila* to study mechanisms of hereditary hearing loss. *Dis. Model. Mech.* **11**, dmm031492. doi:10.1242/dmm.031492

Li, G., Forero, M. G., Wentzell, J. S., Durmus, I., Wolf, R., Anthoney, N. C., Parker, M., Jiang, R., Hasenauer, J., Strausfeld, N. J. et al. (2020). A toll-receptor map underlies structural brain plasticity. *eLife* **9**, e52743. doi:10.7554/eLife.52743

Mackenzie, S. M. and Raible, D. W. (2012). Proliferative regeneration of zebrafish lateral line hair cells after different ototoxic insults. *PLoS ONE* **7**, e47257. doi:10.1371/journal.pone.0047257

Marshall, O. J. and Brand, A. H. (2017). Chromatin state changes during neural development revealed by in vivo cell-type specific profiling. *Nat. Commun.* **8**, 2271. doi:10.1038/s41467-017-02385-4

Marshall, O. J., Southall, T. D., Cheetham, S. W. and Brand, A. H. (2016). Cell-type-specific profiling of protein–DNA interactions without cell isolation using targeted DamID with next-generation sequencing. *Nat. Protoc.* **11**, 1586-1598. doi:10.1038/nprot.2016.084

Matsuo, E., Seki, H., Asai, T., Morimoto, T., Miyakawa, H., Ito, K. and Kamikouchi, A. (2016). Organization of projection neurons and local neurons of the primary auditory center in the fruit fly *Drosophila melanogaster*. *J. Comp. Neurol.* **524**, 1099-1164. doi:10.1002/cne.23955

Morante, J., Erclik, T. and Desplan, C. (2011). Cell migration in *Drosophila* optic lobe neurons is controlled by eyeless/Pax6. *Development* **138**, 687-693. doi:10.1242/dev.056069

Müller, U. and Barr-Gillespie, P. G. (2015). New treatment options for hearing loss. *Nat. Rev. Drug Discov.* **14**, 346-365. doi:10.1038/nrd4533

Nern, A., Pfeiffer, B. D., Svoboda, K. and Rubin, G. M. (2011). Multiple new site-specific recombinases for use in manipulating animal genomes. *Proc. Natl. Acad. Sci. USA* **108**, 14198-14203. doi:10.1073/pnas.1111704108

Obata, F., Tsuda-Sakurai, K., Yamazaki, T., Nishio, R., Nishimura, K., Kimura, M., Funakoshi, M. and Miura, M. (2018). Nutritional control of stem cell division through S-adenosylmethionine in *Drosophila* intestine. *Dev. Cell* **44**, 741-751.e3. doi:10.1016/j.devcel.2018.02.017

Ohlstein, B. and Spradling, A. (2006). The adult *Drosophila* posterior midgut is maintained by pluripotent stem cells. *Nature* **439**, 470-474. doi:10.1038/nature04333

O'Neill, E. M., Rebay, I., Tjian, R. and Rubin, G. M. (1994). The activities of two Ets-related transcription factors required for *Drosophila* eye development are modulated by the Ras/MAPK pathway. *Cell* **78**, 137-147. doi:10.1016/0092-8674(94)90580-0

Ou, H. C., Raible, D. W. and Rubel, E. W. (2007). Cisplatin-induced hair cell loss in zebrafish (Danio rerio) lateral line. *Hear. Res.* **233**, 46-53. doi:10.1016/j.heares.2007.07.003

Papanikolopoulou, K., Mudher, A. and Skoulakis, E. (2019). An assessment of the translational relevance of *Drosophila* in drug discovery. *Expert Opin. Drug Discov.* **14**, 303-313. doi:10.1080/17460441.2019.1569624

Pfeiffer, B. D., Ngo, T.-T. B., Hibbard, K. L., Murphy, C., Jenett, A., Truman, J. W. and Rubin, G. M. (2010). Refinement of tools for targeted gene expression in *Drosophila*. *Genetics* **186**, 735-755. doi:10.1534/genetics.110.119917

Pinto, M. C. X., Kihara, A. H., Goulart, V. A. M., Tonelli, F. M. P., Gomes, K. N., Ulrich, H. and Resende, R. R. (2015). Calcium signaling and cell proliferation. *Cell. Signal.* **27**, 2139-2149. doi:10.1016/j.cellsig.2015.08.006

Podratz, J. L., Staff, N. P., Froemel, D., Wallner, A., Wabnig, F., Bieber, A. J., Tang, A. and Windebank, A. J. (2011). *Drosophila* melanogaster: a new model to study cisplatin-induced neurotoxicity. *Neurobiol. Dis.* **43**, 330-337. doi:10.1016/j.nbd.2011.03.022

Post, Y. and Clevers, H. (2019). Defining adult stem cell function at its simplest: the ability to replace lost cells through mitosis. *Stem Cell* **25**, 174-183. doi:10.1016/j.stem.2019.07.002

Ren, F., Wang, B., Yue, T., Yun, E.-Y., Ip, Y. T. and Jiang, J. (2010). Hippo signaling regulates *Drosophila* intestine stem cell proliferation through multiple pathways. *Proc. Natl. Acad. Sci. USA* **107**, 21064-21069. doi:10.1073/pnas.1012759107

Resende, R. R., Andrade, L. M., Oliveira, A. G., Guimarães, E. S., Guatimosim, S. and Leite, M. F. (2013). Nucleoplasmic calcium signaling and cell proliferation: calcium signaling in the nucleus. *Cell Commun. Signal.* **11**, 14. doi:10.1186/1478-811X-11-14

Ryals, B. M. and Rubel, E. W. (1988). Hair cell regeneration after acoustic trauma in adult Coturnix quail. *Science* **240**, 1774-1776. doi:10.1126/science.3381101

Ryals, B. M., Dent, M. L. and Dooling, R. J. (2013). Return of function after hair cell regeneration. *Hear. Res.* **297**, 113-120. doi:10.1016/j.heares.2012.11.019

Scrucca, L., Fop, M., Murphy, T. B. and Raftery, A. E. (2016). mclust 5: clustering, classification and density estimation using gaussian finite mixture models. *R Journal* **8**, 289-317. doi:10.32614/RJ-2016-021

Shearin, H. K., MacDonald, I. S., Spector, L. P. and Steven Stowers, R. (2014). Hexameric GFP and mCherry reporters for the *Drosophila* GAL4, Q, and LexA transcription systems. *Genetics* **196**, 951-960. doi:10.1534/genetics.113.161141

Singh, A. P., Das, R. N., Rao, G., Aggarwal, A., Diegelmann, S., Evers, J. F., Karandikar, H., Landgraf, M., Rodrigues, V. and VijayRaghavan, K. (2013). Sensory neuron-derived Eph regulates glomerular arbors and modulatory function of a central serotonergic neuron. *PLoS Genet.* **9**, e1003452. doi:10.1371/journal.pgen.1003452

Slattery, E. L. and Warchol, M. E. (2010). Cisplatin ototoxicity blocks sensory regeneration in the avian inner ear. *J. Neurosci.* **30**, 3473-3481. doi:10.1523/JNEUROSCI.4316-09.2010

Southall, T. D., Gold, K. S., Egger, B., Davidson, C. M., Caygill, E. E., Marshall, O. J. and Brand, A. H. (2013). Cell-type-specific profiling of gene expression and chromatin binding without cell isolation: assaying RNA pol II occupancy in neural stem cells. *Dev. Cell* **26**, 101-112. doi:10.1016/j.devcel.2013.05.020

Stone, J. S. and Cotanche, D. A. (2007). Hair cell regeneration in the avian auditory epithelium. *Int. J. Dev. Biol.* **51**, 633-647. doi:10.1387/ijdb.072408js

Su, T. T. (2019). Drug screening in *Drosophila*; why, when, and when not? *Wiley Interdiscip. Rev. Dev. Biol.* **8**, e346. doi:10.1002/wdev.346

Sun, Y., Liu, L., Ben-Shahar, Y., Jacobs, J. S., Eberl, D. F. and Welsh, M. J. (2009). TRPA channels distinguish gravity sensing from hearing in Johnston's organ. *Proc. Natl. Acad. Sci. USA* **106**, 13606-13611. doi:10.1073/pnas.0906377106

Tian, A. and Jiang, J. (2014). Intestinal epithelium-derived BMP controls stem cell self-renewal in *Drosophila* adult midgut. *eLife* **3**, e01857. doi:10.7554/eLife.01857

Vaughan, A. G., Zhou, C., Manoli, D. S. and Baker, B. S. (2014). Neural pathways for the detection and discrimination of conspecific song in D. melanogaster. *Curr. Biol.* **24**, 1039-1049. doi:10.1016/j.cub.2014.03.048

Wagh, D. A., Rasse, T. M., Asan, E., Hofbauer, A., Schwenkert, I., Dürrbeck, H., Buchner, S., Dabauvalle, M.-C., Schmidt, M., Qin, G. et al. (2006). Bruchpilot, a protein with homology to ELKS/CAST, is required for structural integrity and function of synaptic active zones in *Drosophila*. *Neuron* **49**, 833-844. doi:10.1016/j.neuron.2006.02.008

Wang, V. Y., Hassan, B. A., Bellen, H. J. and Zoghbi, H. Y. (2002). *Drosophila* atonal fully rescues the phenotype of math1 null mice: new functions evolve in new cellular contexts. *Curr. Biol.* **12**, 1611-1616. doi:10.1016/S0960-9822(02)01144-2

Warchol, M., Lambert, P., Goldstein, B., Forge, A. and Corwin, J. (1993). Regenerative proliferation in inner ear sensory epithelia from adult guinea pigs and humans. *Science* **259**, 1619-1622. doi:10.1126/science.8456285

White, P. M., Doetzlhofer, A., Lee, Y. S., Groves, A. K. and Segil, N. (2006). Mammalian cochlear supporting cells can divide and trans-differentiate into hair cells. *Nature* **441**, 984-987. doi:10.1038/nature04849

Williams, J. and Holder, N. (2000). Cell turnover in neuromasts of zebrafish larvae. *Hear. Res.* **143**, 171-181. doi:10.1016/S0378-5955(00)00039-3

Yu, H.-H., Chen, C.-H., Shi, L., Huang, Y. and Lee, T. (2009). Twin-spot MARCM to reveal the developmental origin and identity of neurons. *Nat. Neurosci.* **12**, 947-953. doi:10.1038/nn.2345

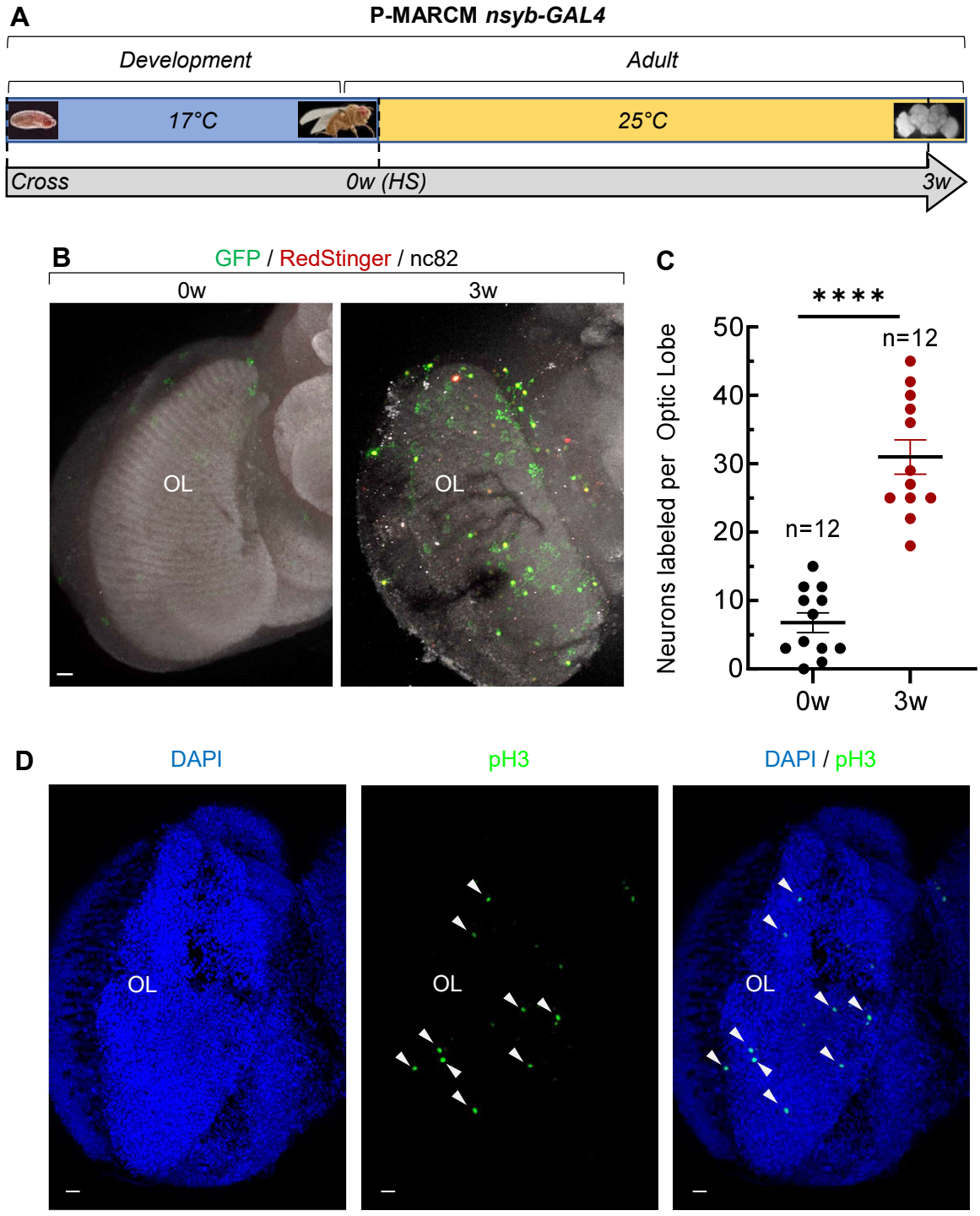

Fig. S1. P-MARCM captures adult neurogenesis in the *Drosophila* optic lobes (OL)

(A) Experimental strategy to reveal adult neurogenesis with P-MARCM *nsyb-GAL4*. Flies 2-5 days–old were Heat-Shocked (HS) to activate the P-MARCM system and brains were dissected 3 weeks (3w) after.

(B) Adult-born neurons in the optic lobes (OL) are labeled by P-MARCM with *nsyb-GAL4* line 3 weeks after HS.

(C) Amount of adult-born neurons in OL at 3 weeks (n=12 OL) is significantly higher than background levels (n=12 OL) (*p=0.0000002,* Student's t-test). Error bars represent s.e.m.

(D) Cell proliferation is also detected by anti-pH3 antibody in the OL (9.2+/-1,0 s.e.m. pH3+ cells/OL; n=26 OL). Scale bars for all panels: 10μm.

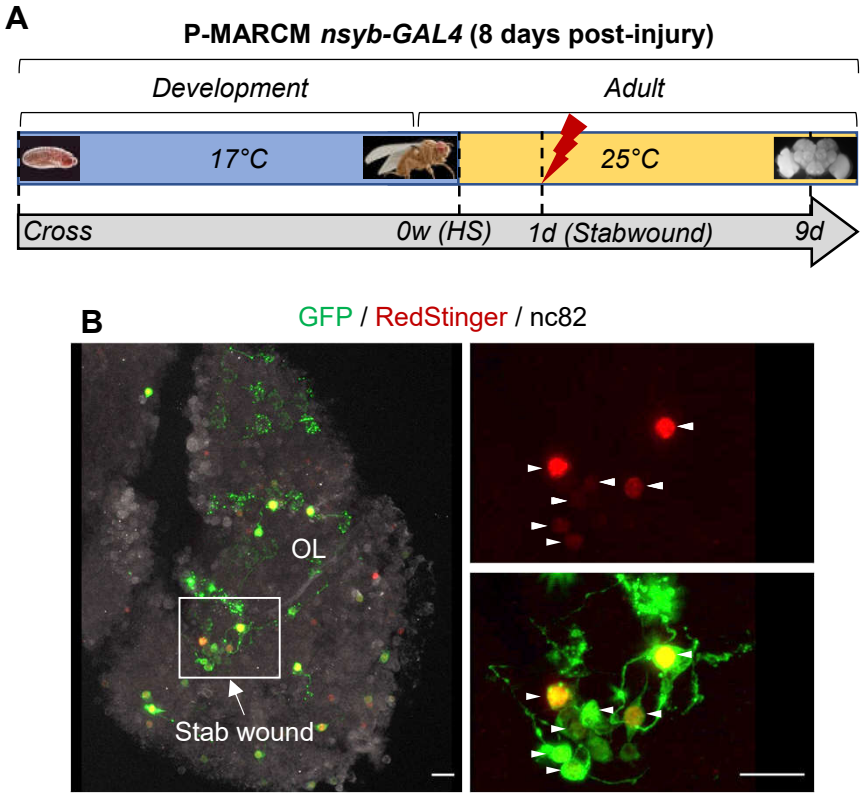

Fig. S2. P-MARCM captures injury-induced neuronal regeneration in the *Drosophila* optic lobe (OL)

(A) Experimental strategy to capture injury-induced neuronal regeneration in OL with P-MARCM *nsyb-GAL4*. Two to 5 days–old flies were Heat-Shocked (HS) to activate the P-MARCM system. Stab wound was applied to the left OL by a fine needle 1 day after HS. Flies were dissected and imaged 8 days later.

(B) Regenerated neurons in the OL (arrowheads) are labeled by P-MARCM with *nsyb-GAL4* line 8 days after stab wound. Scale bar: 10 μm.

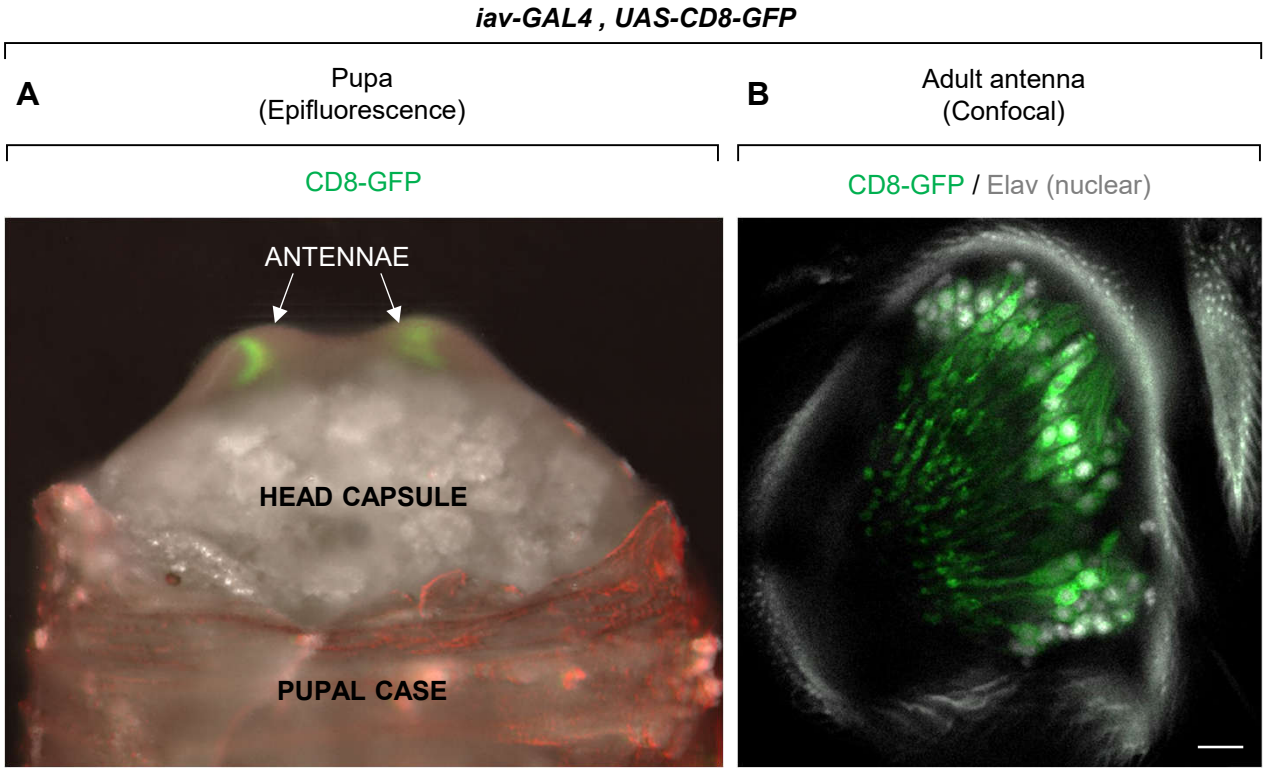

Fig. S3. Expression pattern of *iav-GAL4* line in the antennae.

(A) Expression of *iav-GAL4* in the antennae begins in pupal stage.
(B) *iav-GAL4* expression is restricted to JO neurons in adult antenna. Scale bar: 10μm.

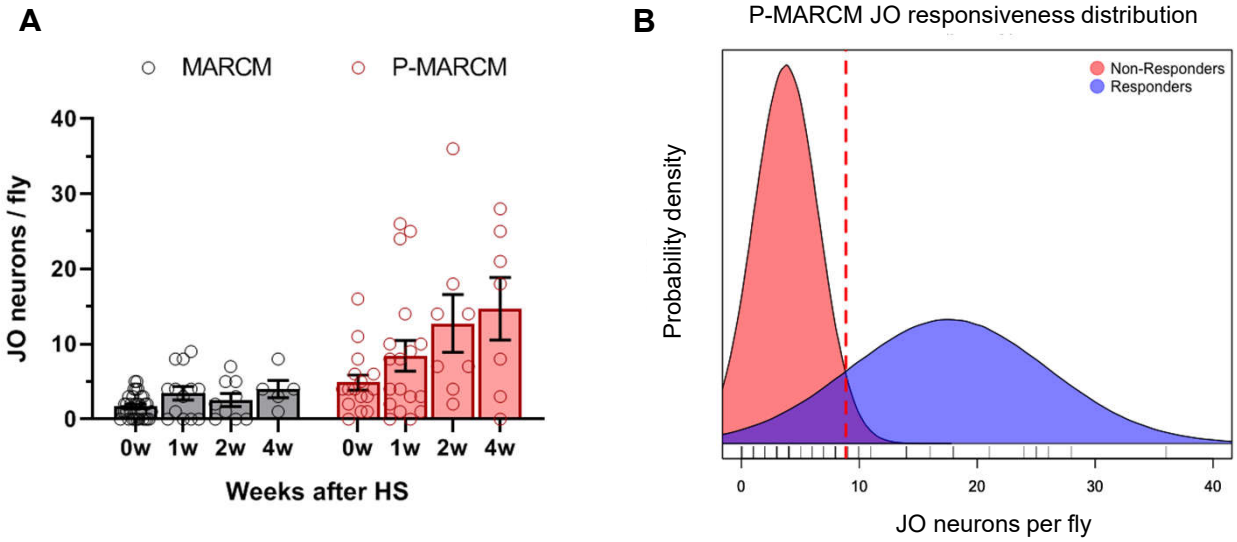

Fig. S4. JO neurogenesis detection and distribution

(A) Quantification of newborn JO neurons in MARCM and P-MARCM lineage tracing approaches. JO neurogenesis increases over time upon P-MARCM labeling. Error bars represent s.e.m.

(B) Gaussian mixture model classifies flies into “Responders” and “Non-responders” indicating the presence of adult JO neurogenesis beyond background levels.

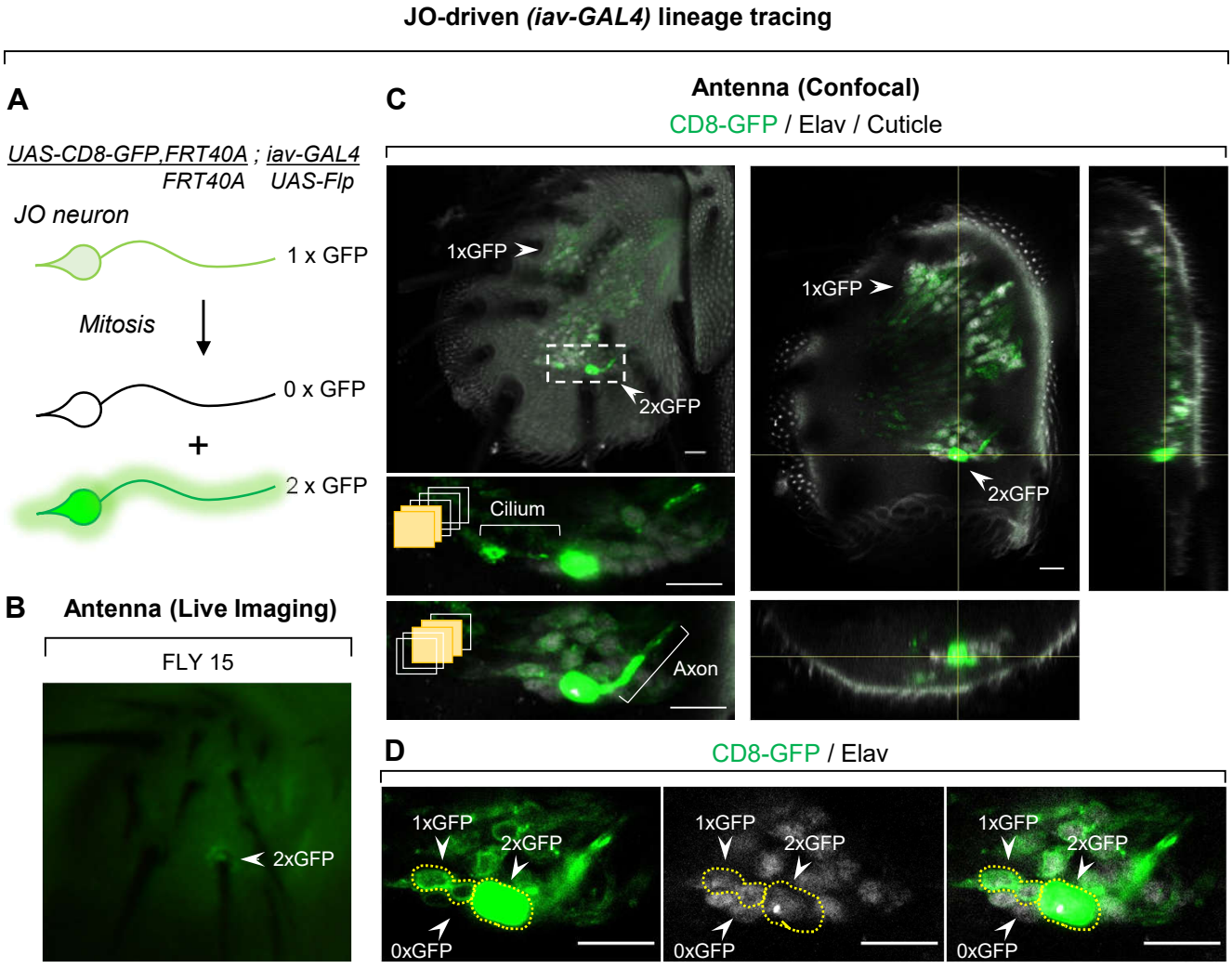

Fig. S5. Neurogenic clones from JO neurons are captured at single-cell resolution *in vivo*.

(A) *.iav-GAL4*-driven lineage tracing system to assess neurogenesis from JO neurons. Daughter cells express 2xGFP and 0xGFP, while non-dividing JO neurons contain 1xGFP.
(B) A single JO neuron expressing 2xGFP detected by fluorescent microscopy on an intact, alive fly.
(C) Confocal microscopy confirms proliferation of a single neuron on the anterior part of the antenna. Captions show maximum intensity projections of discrete planes to visualize the JO neuron cilium and axon.
(D) Neurogenesis from JO neurons detected by twin-spots of 2xGFP/Elav+ neurons and 0xGFP/Elav+ neurons among non-dividing 1xGFP/Elav+ JO neurons. Scale bars: 10μm

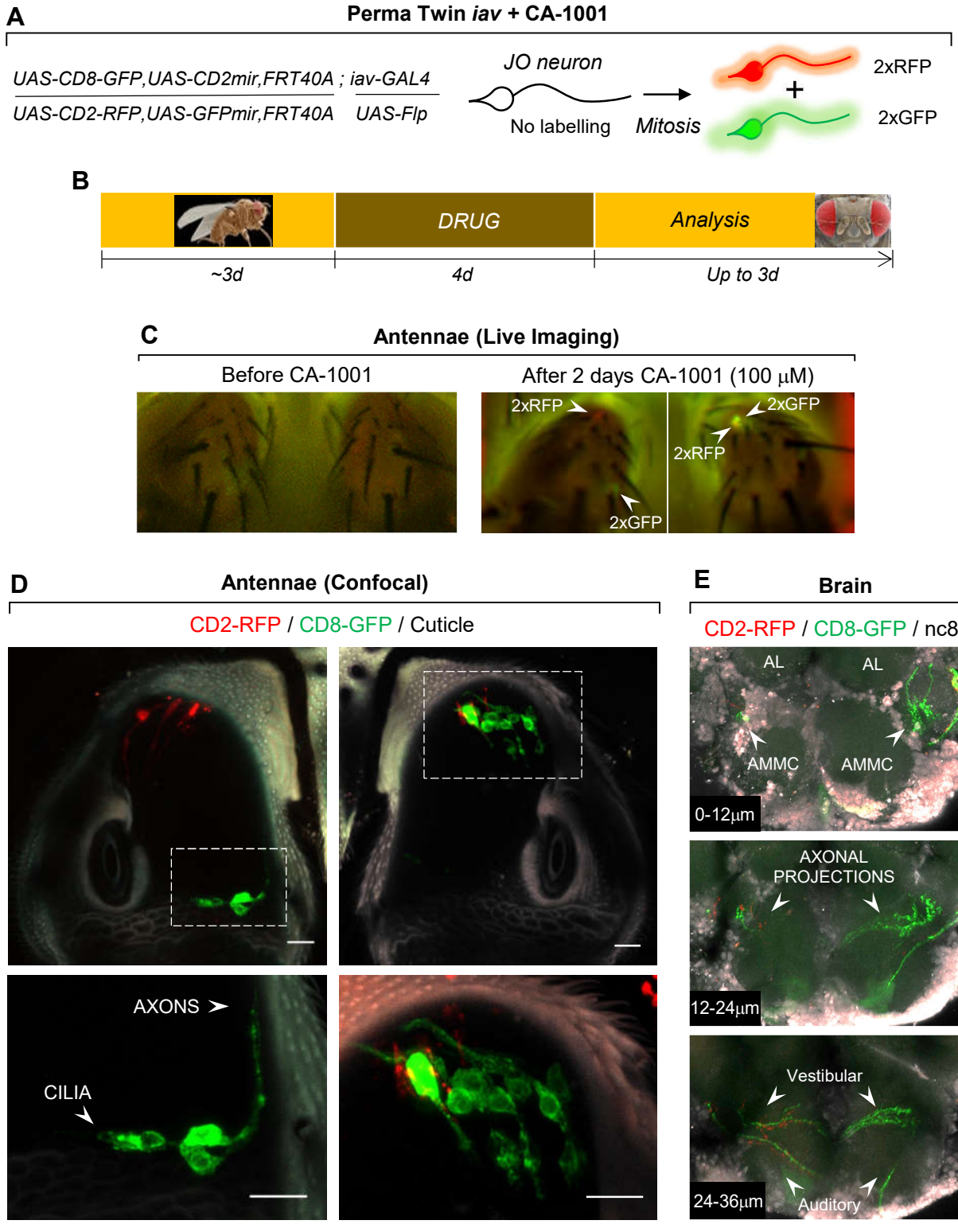

Fig. S6. The calcium ionophore CA-1001 increases neurogenesis from JO neurons.

(A) Perma Twin-iav lineage tracing system to assess neurogenesis from JO neurons.
(B) Experimental strategy to capture neurogenesis from JO neurons. Three-day old PT-iav flies receive oral drug administration for 4 days and are analyzed up to 3 days later.
(C) New JO neurons are detected by fluorescent microscopy on intact, alive flies as soon as 2 days after administration of CA-1001 at 100μM.
(D) Newly-generated JO neurons develop cilia and extend axons to the brain. AMMC: Antennal Mechanosensory and Motor Center; AL: Antennal Lobe
(E) New JO neurons target the brain in the Auditory and Vestibular circuit pattern as early as 2 days following drug administration. Scale bars for all panels: 10μm.

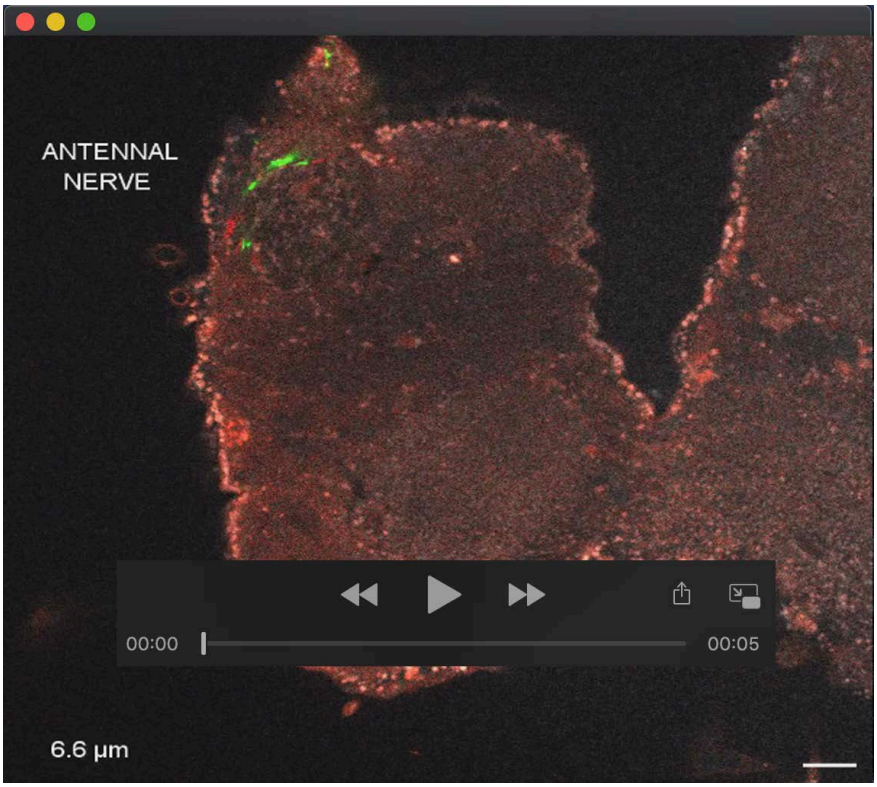

Movie 1. Axonal projections of regenerated Johnston Organ (JO) neurons induced by CA-1001. Annotated confocal stack of newborn auditory and vestibular JO neuron axonal projections after 2 days of CA-1001 administration to Perma Twin-iav flies. Scale bar: 10 mm.